Palladium-Based Metal Organic Frameworks as Heterogeneous Catalysts for C-C Couplings

Arputham Shophia Lawrence,[$a] Nuria Martin,[$b] Balasubramanian Sivakumar,[a] Francisco G. Cirujano*[b, c] and Amarajothi Dhakshinamoorthy*[d]

[a]School of Mathematics, Madurai Kamaraj University, Madurai, Tamil Nadu, 625 021, India.

[b]Institute of Molecular Science (ICMOL), Universidad de Valencia, 46980 Paterna, Valencia, Spain. E-mail: francisco.c.garcia@uv.es
[c]Departamento de Química Inorgánica y Orgánica, Universidad Jaume I, 12071 Castellón, Spain. E-mail: cirujano@uji.es

[d]School of Chemistry, Madurai Kamaraj University, Madurai, Tamil Nadu, 625 021, India
E-mail: admguru@gmail.com; adm.chem@mkuniversity.org
$: Both authors contributed equally

Abstract

Among the various cross coupling reactions, C-C cross coupling reaction has attracted many researchers to investigate for the last four decades. The continuous, constant and consistent progress in this field fetched a Noble prize in 2010, showing the importance of this reaction in diversified fields. Among the various transition metals studied for this reaction, Pd is one of the metals that have exhibited the highest activity due to its unique features and reactivity. Although Pd-based homogeneous catalyst was the preferred choice for many researchers, the field slowly diverted towards the development of Pd-based heterogeneous catalysts for C-C coupling reaction. This is obviously due to the high cost of Pd precursor, its self-deactivation. In this context, metal organic frameworks (MOFs) are one of the solid catalysts frequently employed as host matrix for the deposition of Pd(II) salts and Pd nanoparticles. This is due to the widespread possibilities available for the functionalization of MOFs and their stability during the synthetic procedure. This review provides the design and development of Pd-based MOFs as heterogeneous catalysts for the C-C cross coupling reaction. After a brief introduction on MOFs and the importance of C-C coupling reaction, the main part of the review summarizes the catalytic data with respect to Pd(II) and Pd nanoparticles as active sites. The last section provides our views in this field for the further development in the near future.

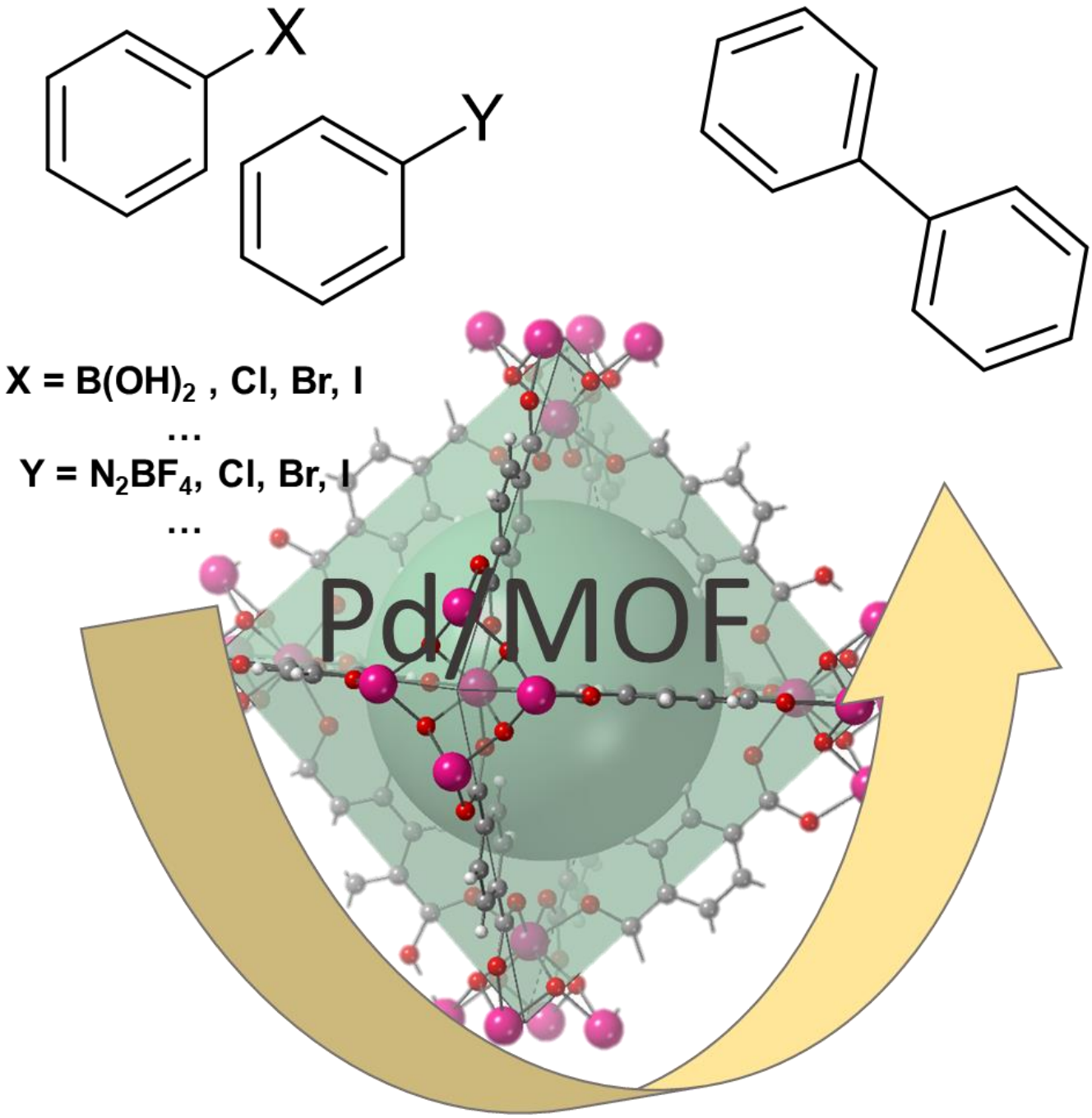
X
Y
X = B(OH)2 , Cl, Br, I
…
Y = N2BF4, Cl, Br, I
…
Pd/MOF

1. Introduction

The formation of C-C bonds using palladium (such as Suzuki or Heck couplings of boronic acids and/or halides) is a ubiquitous reaction in organic synthesis and catalysis for the construction of molecules with industrial and thus societal interest, such as bulk chemicals, fine chemicals and pharmaceuticals.[1-10] The development and use of noble metals for the safe, robust and sustainable production of pharmaceutically relevant molecules, through catalytic C-C couplings, is a challenge of the academic and industrial chemical communities. Among the various transition metal based catalysts,[11-13] Pd-based catalysts exhibit the highest activity in the cross coupling reactions. For instance, the use of Pd-based catalyst in the cross coupling between different types of organoboron derivatives with organic electrophiles (halides, triflates) using a base provide a convenient and straightforward strategy to construct C-C bonds. Scheme 1 provides various organoboron compounds reported for the cross coupling reactions with series of electrophiles of organic compounds.

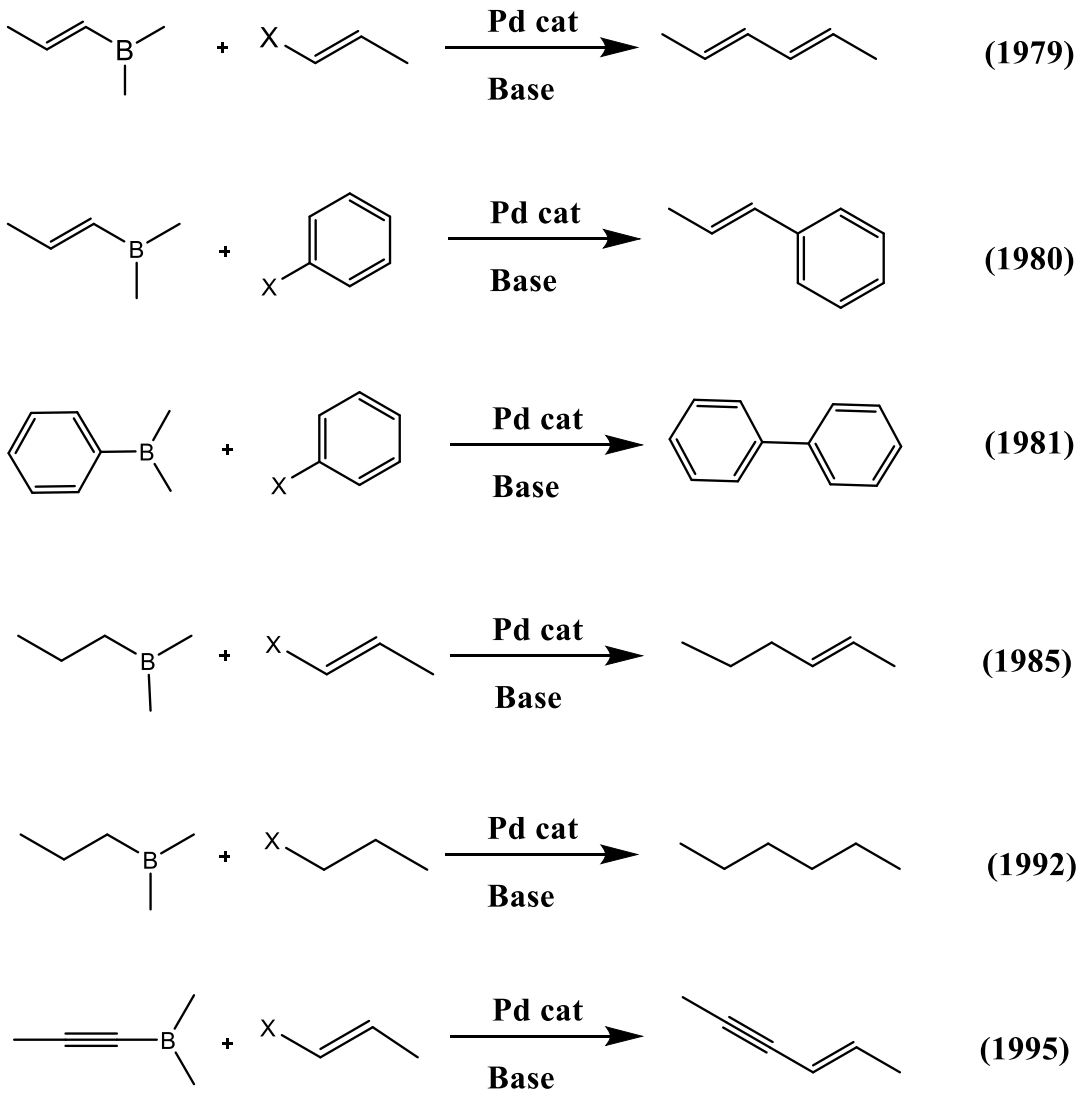

Scheme 1. Representative cross coupling C-C bond forming reactions between various organoboranes with series of organic electrophiles. Years in parentheses suggest the reported years by Suzuki and co-workers.

As discussed above, these reactions have been reported by many research groups in the last four decades especially in the preparation of fine chemicals, organic molecules and natural products.[14-17] This has been the topic of interest for many groups since this reaction affords the following advantages. They are

- Readily available reactants
- Milder experimental conditions with high yields
- Stability of catalysts in water
- Reaction may be performed in aqueous and heterogeneous medium
- Broad range of functional groups tolerance
- High regio-/stereoselectivity
- Small amount of catalysts is sufficient
- Applicable in one-pot synthesis
- Easy separation boron compound (inorganic)
- Environmentally friendly process

The recent advances in heterogeneous catalyst design for surpassing activity, selectivity and specially, stability of their homogeneous counterparts are based in the isolation of the Pd active sites in a solid support by anchoring through different type of bonds.[18-25] In this aspect, one of the solids that has attracted researchers in the last two decades is metal organic frameworks (MOFs). They are porous crystalline solids whose crystal network is formed by the coordination between metal ions/clusters with rigid organic linkers.[26-28] Among the various properties of MOFs, high surface area[29] and porosity[30] are playing a crucial role in heterogeneous catalysis mainly to facilitate adsorption/desorption processes. On the other hand, the active sites in MOFs can be facilely tuned by the selection of appropriate synthesis procedures.[31] Some of the most frequently employed active sites in heterogeneous catalysts are Lewis acids/Brönsted acids,[32-34] Brönsted base[35, 36] and MOFs as hosts for metal nanoparticles (NPs)/complexes.[37-43] One of the attracting features of MOFs compared to other related porous solids is that MOFs can be subjected to post-synthetic modification (PSM) to alter the functional groups either at linker or at metal nodes.[44-46] In this aspect, MOFs appear as versatile multifunctional platforms to graft Pd active sites either at the pores, organic functional groups or inorganic nodes, allowing the site isolation (and multiplication of turnovers due to minimization of self-deactivation) and stabilization in a solid heterogeneous platform.[47-50]

Different MOF structures have been employed for the grafting of Pd active sites, being the most widely used the UiO-66/67 and MIL-101 families due to their high porosity, crystallinity and stability. Both MOFs are prepared from 1,4-benzenedicarboxylic acid (BDC or terephthalic acid), known as the linker, and tetravalent or trivalent metal (Zr^{4+}, Hf^{4+}, Ce^{4+} or Cr^{3+}/Fe^{3+}/Al^{3+}) ions, for the UiO and MIL-101 families, respectively. Under solvothermal conditions of temperature (e.g. 60-180 ºC) in polar solvents (e.g. DMF, water) with the presence of crystal-growth modulators (e.g. acids), metal-linker coordination bonds are formed by self-assembly resulting in 12-connected $Zr_6O_4(OH)_4$ or trimeric Cr_3O octahedral clusters, also known as secondary building units or SBUs. The crystal growth result in 3D

highly porous frameworks with periodic structure and compositions with chemical formulas of $Zr_6O_6(BDC)_6$ and $Cr_3F(H_2O)_2O(BDC)_3$, for UiO-66(Zr) and MIL-101(Cr), respectively. On the one hand, the UiO-66 structure contains a tetrahedron cage of 7.5 Å, an octahedron cage of 12 Å and a pore aperture of 6 Å. On the other hand, the MIL-101 structure contains two mesoporous cages with diameters of 29 and 34 Å accessible through a small pentagonal window of 12 Å, as well as large pentagonal and hexagonal windows of 14.7 by 16 Å free aperture. This porous space, together with the possibility of introducing functional groups in the organic linker (e.g. $-NH_2$) allows the grafting of Pd complexes or nanoparticles inside the porous cavities of both MOFs.

As commented earlier, Pd can be grafted to any one of the active sites available in MOFs.[51] The Pd(II) or Pd NPs incorporated within the MOF can be characterized by series of analytical/morphological techniques. For instance, powder X-ray diffraction provides the formation of MOF structure and its crystallinity. During the process of grafting Pd(II) or Pd NPs over MOFs, it is very often ascertained that the crystallinity and peak intensity/position remain unaltered as in the case of pristine MOF. Furthermore, the loading of Pd in the Pd incorporated MOF is determined by ICP analysis. FT-IR is very much useful to prove the interaction of Pd(II) with the active sites either at the metal node or at the satellite positions in the linker. Gas adsorption/desorption measurements were performed to confirm the loading of Pd(II) or Pd NPs. The decrease in the BET surface area and porosity of MOF solids upon increasing the loading of Pd is often considered as a direct evidence of for the successful incorporation of Pd. One of the crucial issues in the introduction of Pd(II) sites within the MOFs is to retain its oxidation state during the loading process. In some case, the oxidation state of Pd(II) was reduced to Pd NPs which can be distinguished by XPS studies. Similarly, XPS can also provide concrete evidence for the presence of Pd NPs. On the other hand, TEM images show the presence and uniform distribution of Pd NPs throughout the framework.

One of the highest benefits of heterogeneous catalysts compared to homogeneous catalysts is their easy recovery from the reaction medium and to reuse in consecutive cycles. The activity of a solid catalyst is often represented by turnover number (TON) or turnover frequency (TOF) and in some cases, conversion/yield is also reported. In order to achieve identical activity of a heterogeneous catalyst in consecutive reuses, the density and quality of active sites must be retained as in the case of a fresh catalyst. One of the convenient methods to determine the stability of a heterogeneous catalyst is to check the leaching (hot filtration test) of active sites and reusability tests. Characterization of the reused solid catalysts by the above commented techniques and comparing these results with the fresh solid catalyst would certainly provide strong evidences for the stability of heterogeneous catalyst. In addition, these comparison data also highly useful to understand catalyst deactivation.

Large efforts have been taken during last years in the design of Pd based MOFs as heterogeneous catalysts for C-C coupling reactions, which are summarized in the present review, paying attention on the location and type of Pd active site immobilized in MOFs. On the one hand, molecular Pd complexes have been presented, which are in turn classified based on the precise framework location of the sites. On the other hand, Pd NPs on MOFs are reviewed in terms of their potential as solid catalyst in important C-C bond forming reactions. The review is concluded with the prospect of using MOFs as high performance catalytic system for the coupling of carbon atoms in an environmentally friendly manner.

2. Molecular Pd complexes on MOFs

The following sections provide the activity of Pd(II) anchored over MOFs solids by adsorption over metal nodes, through the chemical interaction with the inorganic nodes, coordination with bipyridine sites, coordination at Schiff base sites and interaction with N-heterocyclic carbenes. These are the different strategies that have been reported in the literature to isolate the active Pd(II) sites for C-C coupling reactions. Due to the presence of high surface area in MOFs, the anchoring of Pd(II) sites by any of the above methods favour the site isolation and avoiding self-deactivation.

2.1 Physical adsorption at the pores

Dangling carboxylate bonds present in the Zn-benzenetricarboxylate containing MOF-5 served as anchoring points for $Pd(OAc)_2$, which exchanged one acetate ligand by the carboxylic group from the MOF linker under room temperature conditions in dichloromethane.[52] This resulted in a loading of 2.3 wt% Pd, maintaining the crystallinity and surface area of the MOF with a BET value of 2570 $m^2 g^{-1}$. The solid was active (5 mol% Pd) in the C-H phenylation of naphthalene using diphenyliodoniumtetrafluoroborate (Scheme 2) at 120 ºC in nitrobenzene obtaining 64% yield (TON: 13) which is relatively higher with 13% yield (TON: 3) obtained with the homogeneous $Pd(OAc)_2$. Unfortunately, the reaction conditions degraded the MOF framework as shown by powder XRD analysis and the Pd(II) aggregates into Pd NPs (evidenced by TEM study).

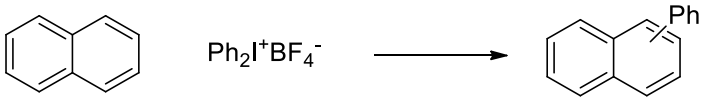

Scheme 2. Direct phenylation of naphthalene.

The reaction between 4-iodoaniline and $Na_2[PdCl_4]$ afforded the complex (trans-dichlorobis(4-iodoaniline-*κ*N)palladium(II)) which was encapsulated within the nanocages of MIL-101 (1.4% Pd loading) through Ship-in-a-bottle approach.[53] The XRD pattern of the MOF was maintained during this process, however, the BET surface area decreased from 2730 to 1418 $m^2 g^{-1}$ upon loading the complex. Furthermore, good dispersion of square planar Pd(II) complex has been proved by energy dispersive X-ray (EDX) and X-ray photoelectron spectroscopy (XPS) analysis. The Pd-MOF was an active catalyst (0.06 mol% Pd) in the Suzuki-Miyaura coupling between 4-iodoanisole and phenylboronic acid at room temperature in ethanol/water using K_2CO_3 as the base.[53] The product yield of 96% was obtained after 15 min (TON: 1620, TOF: 1820 h^{-1}) with the encapsulated complex at the MOF. In contrast, 25% yield (TON: 420, TOF: 830 h^{-1}) of the product was obtained with the bulk complex after 30 min. The Pd-MOF was reused in six runs with less than 2% Pd leached, but all the Pd was converted to Pd NPs (according to XPS and TEM analysis). The Pd-MOF was also active (0.5 mol% Pd) in the Heck coupling between 4-iodoanisole and styrene at 80 ºC in DMF/water using K_2CO_3 as the base giving 94% yield after 4 h (TON: 190).

Phosphine palladium complexes of $PdCl_2P_2$ were encapsulated in the nanocages of NiL MOF (L= L=4,4′-(benzene-1,4-diyldiethyne-2,1-diyl)bis(1-H-pyrazole) (Figure 1), resulting in a decrease of BET surface area form ca. 3000 to 2000 $m^2 g^{-1}$, while maintaining the MOF crystallinity and Pd (II) oxidation state.[54] The host-guest supramolecular

architecture was employed as catalyst (1 mol% Pd) in the Heck coupling between iodobenzene and estragole (Scheme 3), resulting in 76% conversion in DMF at 110 ºC, using K_2CO_3 as the base. However, the conversion decreased to 53% after the 3rd run, due to the leaching of the complex (decreasing the Pd loading to 0.04%)

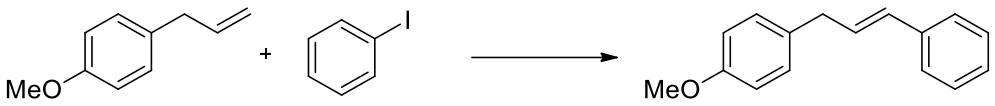

Scheme 3. Heck coupling between estragole and iodobenzene.

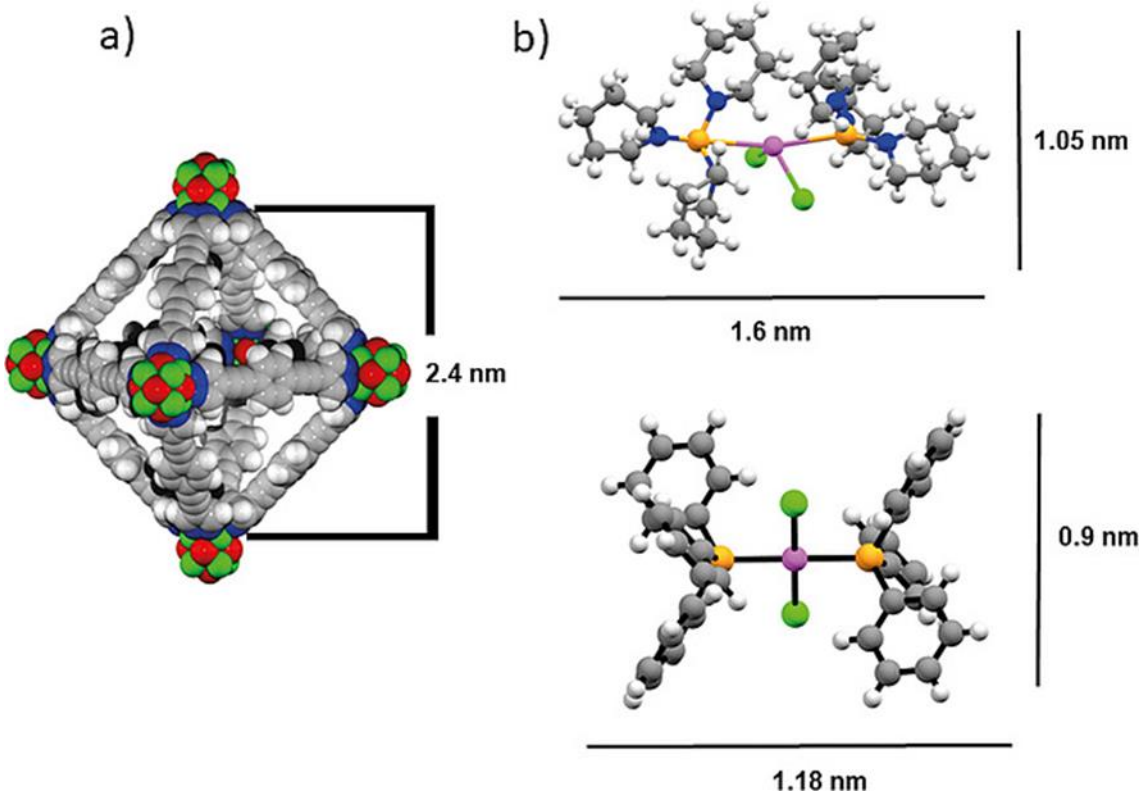

Figure 1. View of the octahedral voids in the structures of (a) the Ni-MOF and (b) the Pd-1 (above) and Pd-2 (below) complexes. Reproduced with permission of ref. [54] Copyright 2019 Wiley.

UiO-66 with free carboxylic acid sites at the linker was employed as a host of $Pd(OAc)_2$ (1 mol% Pd) for the coupling between 1-methylindole and diphenyliodonium tetrafluoroborate (Scheme 4) in γ-valerolactone at 80 ºC, resulting in 94% yield (TON: 94) after 5 h, with respect to the 40% yield obtained with bulk $Pd(OAc)_2$.[55] The interaction and ligand (-OAc/-CO_2H) exchange of the palladium acetate at the carboxylic acid linkers was proved by X-ray absorption fine structure (EXAFS) analysis. The catalyst was successfully recycled 4 times with no decrease in crystallinity or yield and Pd leaching was below 7 ppm. However, reduction of Pd(II) to Pd(0) and migration to the surface of the MOF was observed by TEM, as a probable cause of deactivation, although those NPs were highly dispersed due to the effect of the carboxylic acids of the MOF.

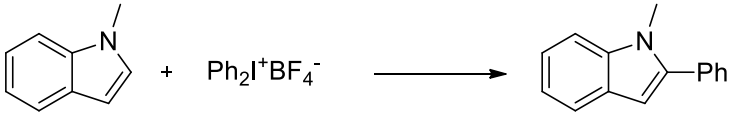

Scheme 4. Selective arylation of indole with aryl iodonium salts.

The encapsulation of 5 mol% of $Pd(OAc)_2$ in the Cu-MOF-74 resulted in the increment of the lifetime of Pd(II) active sites, due to the re-oxidation of the Pd(0) formed during the alkenylation of indole with butyl acrylate (TON: ~15), with respect to the TON of ca. 5 obtained with bulk $Pd(OAc)_2$.[56] The crystallinity of the MOF was maintained; however, the Pd(II) eventually got reduced into Pd(0), without activity in additional reaction cycles.

Na_2PdCl_4 was encapsulated over MIL-88B-NH_2(Cr), resulting in a loading of 9.2 wt% Pd, and employed as a heterogeneous catalyst (0.1 mol%) in the homocoupling of p-tolylboronic acid at room temperature and 1 bar of oxygen in ethanol/water using sub-stoichiometric amount of Cs_2CO_3 as the base.[57] A yield of 69% (TON: 909) was obtained with the Pd-MOF, which maintained the XRD pattern after five reaction runs, although the activity decreases after the first recycle due to the formation of Pd NPs with increased size upon recycling (observed by TEM). An oxidation treatment with potassium peroxodisulfate in 2 M HCl, restored the activity of the Pd(II)@MIL-88B-NH_2 decreasing the number of Pd(0) clusters without modifying the MOF structure.

2.2 Chemical bonding to the inorganic nodes

In one of the earlier reports, $[Pd(2\text{-pymo})_2]_n$ (pymo: 2-hydroxypyrimidinolate) MOF (32 wt% Pd content and 600 $m^2\,g^{-1}$ BET surface area), with a regular micropore structure (Figure 2) was prepared from 2-hydroxypyrimidinolate and K_2PdCl_4 and employed as a heterogeneous catalyst (2.5 mol% Pd) in the Suzuki-Miyaura cross C-C coupling of p-bromoanisole and phenylboronic acid in o-xylene at 150 ºC using K_2CO_3 as a base.[58] A yield of 85% after 5 h was achieved, resulting in a TON value of 34 using high reaction temperatures (i.e. 150 ºC) and a large excess of base (c.a. 6 eq.). In an experiment with a Pd loading of 10 times lower, the calculated TOF was 1230 h^{-1}. Despite the Pd(II)/Pd(0) re-oxidation cycle taking place during the mechanism, the bulk MOF withstands the reaction conditions and was reusable (only one recycle) when the reaction was performed at room temperature (ca. 90% yield after 48 h after the second run).

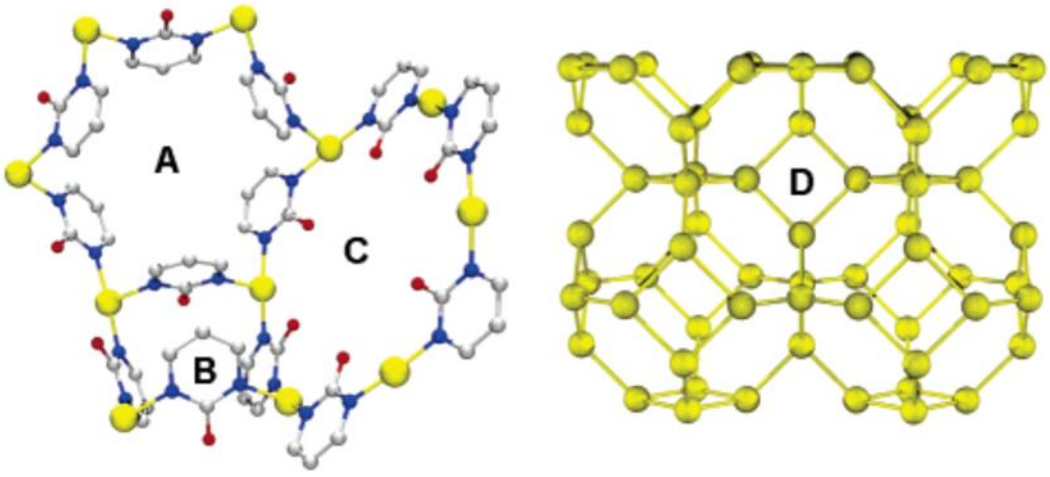

Figure 2. Structural motives found in the crystal structure of $[Pd(2\text{-pymo})_2]_n$: metallacalix[6]arene (A), metallacalix[4]arene (B), and planar molecular hexagon (C). Pd: yellow. O: red. N: blue. C: gray. D shows the zeotype sodalite framework. Reproduced with permission of ref.[59] Copyright 2006 American Chemical Society.

The same MOF (3 mol% Pd) was employed as heterogeneous catalyst in the Suzuki-Miyaura coupling between arenediazonium ion and phenylboronic acid (Scheme 5) in methanol at 40 ºC, yielding 99% of the product (TON: 33),[60] while neither the Pd precursor or linker promotes the reaction (0% yield). The MOF was reused three times with a noticeable decrease in activity after the 4th run, indicating reduction of Pd(II) to Pd(0) and collapse of the structure.

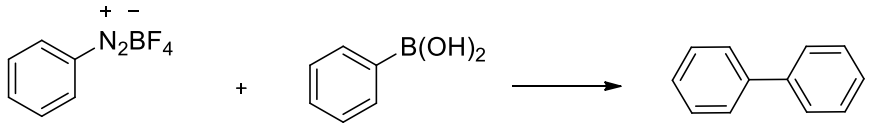

Scheme 5. C-C coupling between arenediazonium ion and phenylboronic acid.

A different azolate-palladium MOF containing Ln-carboxylate moieties as well in the structure was proposed as N-Pd-N active nodes (0.2 mol%) for the Suzuki-Miyaura coupling between bromobenzene and phenylboronic acid at 50 ºC in ethanol/water, using K_2CO_3 as a base.[61] This resulted in 99% yield after 4 h (TON: ~ 500). Eight cycles were performed by maintaining the yield as high as 90 %. Although Pd(II) was reduced as evidenced by TEM and XPS analysis, no leaching of Pd was observed.

Zr-MOF-808 with coordinatively unsaturated sites at the node in which $Pd(OAc)_2$ coordinated to the Zr-oxo clusters via Zr-OH/Zr(PdOAc) exchange as evidenced by X-ray absorption and IR analysis. This solid was employed as a catalyst in the oxidative Heck homocoupling of o-xylene.[62] The Pd-MOF (0.05 mol%Pd) was active at 110 ºC for 17 h, under oxidative (16 bar O_2) acid (acetic acid/propane sulfonic acid) conditions, resulting in a TON > 400 for 3 reaction runs, with only 2% Pd leaching after the 1st run and 5%Pd leached after the 3rd run, resulting in a cumulative TON> 1200.

Sulfated and phosphated Hf_6-oxide nodes of MOF-808 served as anchoring points of Pd(II), which got stabilized at such points after post-synthetic modification (PSM) of the MOF with $Pd(OAc)_2$, minimizing the formation of Pd NPs, as checked by XPS and TEM.[63] The PdMOF (5 mol%Pd) was tested in the oxidative Heck reaction between 2-phenylphenol and ethyl acrylate in 2-methylbutanol at 100 ºC, using triethylamine (TEA) as a base and $Cu(II)/O_2$ as the oxidant, achieving a TOF of ca. 1 h^{-1} and 50% yield after 48 h (TON: 25). The loss in activity during the course of the reaction was due to the formation of Pd NPs, which may inactivate the heterogeneous catalyst since no reuses were provided.

3. Chemical bonding to chelating organic functional groups at the linkers

3.1 Pd at bipyridine sites

One of the first reports on using bipyridyl sites in a MOF to graft Pd as catalytic site for C-C couplings was the palladium-yttrium bimetallic MOF prepared from K_2PdCl_4, where the Pd atoms (with +2 oxidation state according to XPS) is coordinated (with a square planar *cis*-type geometry) to the two nitrogen atoms of the bipy linker and two chlorine atoms. The MOF was employed as a catalyst (0.11 mol% Pd) in the Suzuki-Miyaura coupling between 4-methylphenylboronic and iodobenzene at 80 ºC in water for 8h, using K_2CO_3 as a base.[64] A 96% yield of the 4-methylbiphenyl was obtained (TON: 890) with the Pd-MOF, which is similar to the activity of $Pd(OAc)_2$, but slightly higher than the homogeneous $Pd(bipydc)Cl_2$ (65%, TON: 601) for the same reaction time. However, diffusion limitations to the narrow micropores of the MOF (ca. 0.3 nm) disfavoured the conversion of bulkier aryl iodides. Similar results were observed for the Sonogashira coupling using DBU as the base, under

the same reaction conditions. The catalysts withstand the reaction conditions and could be successfully recycled in 5 runs, with minor changes in the Bragg intensities of the XRD (due to pore blocking) and no leaching of Pd or changes in its oxidation state (no NP or Pd black formation) according to XPS, highlighting the strong stabilizing effect of the bipy (as well as site-isolation provided by the framework).

Xiu et al. introduced extra-long hydrophobic alkyl chains in the biphenyl ring of the UiO-67 MOF, close to coordination environment of the hydrophilic Zr_8O_8 metal-oxoclusters, resulting in superhydrophobic/oleophilic MOFs with the same crystallinity to the pristine MOF (see Figure 3).[65] The BET surface area decreased from 1303 to 349 $m^2 g^{-1}$ as the alkyl chain increased from C_2 to C_8, values much lower than pristine UiO-67 (2761 $m^2 g^{-1}$), although the pore sizes were similar (ca. 1.1 nm). When the MOFs were soaked in acetonitrile at 65 ºC in the presence of $PdCl_2(CH_3CN)_2$ for one day, resulting in Pd loadings between ca. 3.4 and 7.7 wt% Pd (analysed by ICP), when increasing the 2,3'-bipyridine-5,6'-dicarboxylic acid linker amount from 36 to 61 wt.% in the MOF containing the C_8 chain. This corresponds to the quantitative metalation of all the bipy linker sites, without affecting the MOF crystalline structure or +2 oxidation state of Pd, assessed by XRD and XPS, respectively. The materials were examined as catalysts (1 mmol% Pd) in the room temperature aqueous Sonogashira reaction between phenylacetylene and iodobenzene using TEA as a base. After 5 h, the yields and TOFs increased from 44% (TOF: 9 h^{-1}) to ca. 91% (TOF: 18 h^{-1}) for UiO-67 (36 wt.% bipy) without or with the C_8-functionalized linker, respectively, highlighting the key role of the hydrophobic active site environment in the water medium. When increasing the amount of Pd-bipy, from 36 to 48 and 61 wt% (with the subsequent increase in Pd), the yields and TOFs decreased from 91% (TOF: 18 h^{-1}) to 85% (TOF: 17 h^{-1}) and 77% (TOF: 15 h^{-1}), respectively, probably due to the lower porosity and less site-isolation of Pd active sites. The values are comparable to that of 79% yield (TOF: 16 h^{-1}) for the homogeneous $Pd(CH_3CN)_2Cl_2$. However, the super-hydrophobic MOF could be recycled ten times, maintaining the product yield >85% and the crystalline structure and Pd content (no leaching measured and no activity detected after a hot filtration test). In contrast, the pristine UiO-67-bipy-Pd decreased the product yield from 44 to 10% after the first reaction run, leaching 0.13 $mg \cdot L^{-1}$ (ICP measurements) and collapsing the crystalline framework during the reaction as shown from XRD and TEM analysis.

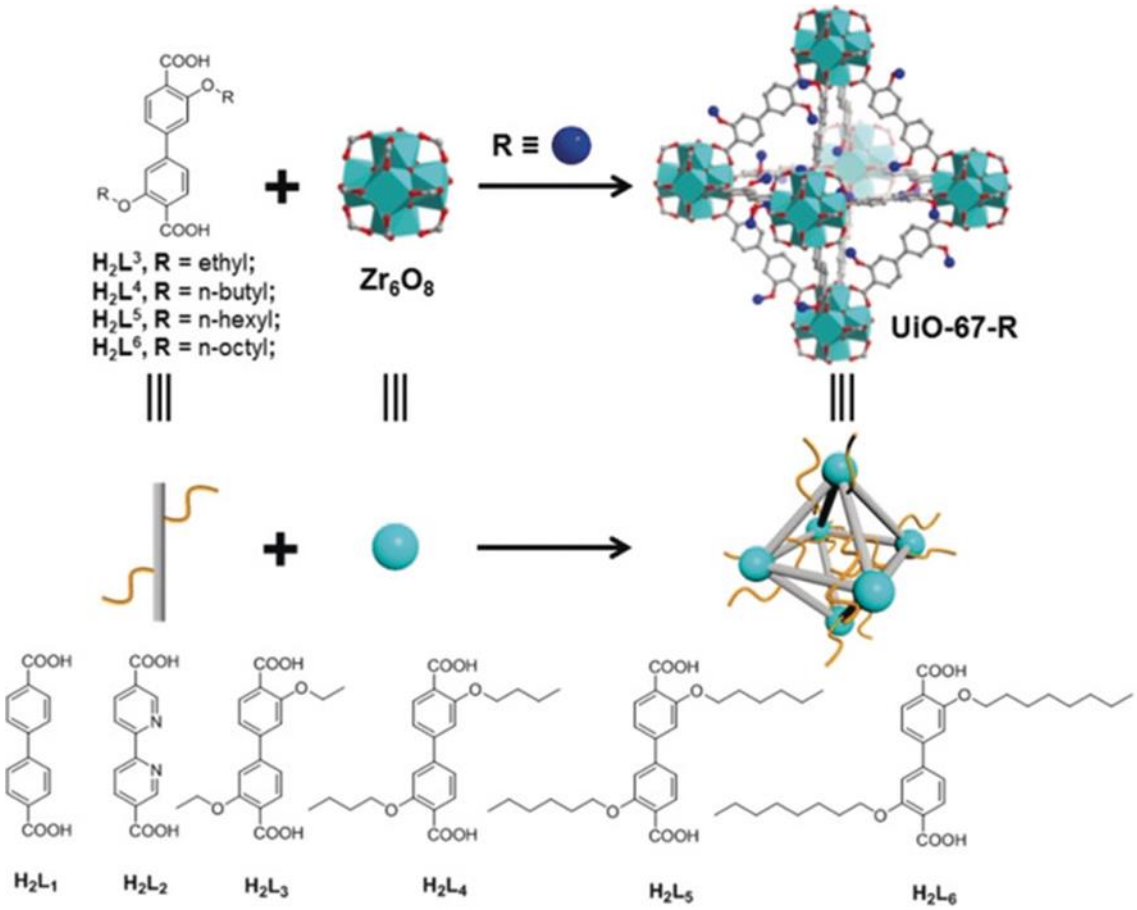

Figure 3. Construction of **UiO-67-R**s from Zr_6O_8 clusters and $\mathbf{H_2L}^{n}$ (n = 3–6) linkers containing alkyl chains. Reproduced with permission of ref.[65] Copyright 2019 Wiley.

The introduction of similar $PdCl_2(CH_3CN)_2$ complex at the UiO-67-bipy resulting in a loading of 1 wt.% Pd in the form of Pd(II) with slightly higher electron density from the bipy-N atoms (ca. 3.7% of the bipy linkers coordinated to $PdCl_2$), with respect to the homogeneous $PdCl_2(CH_3CN)_2$ (as seen by the XPS shifts).[66] Those sites were catalytically active (0.2 mol% Pd) in the carbonylative Sonogashira coupling between 4-methoxyiodobenzene, phenylacetylene and CO using Cs_2CO_3 as a base at 100 ºC in DMF for 6 h, resulting in 95% yield of the product (TON: 475). The MOF was recycled five times, with no loss in its activity or crystallinity, and only minimum Pd leaching (<0.2% of the total Pd) in line with the hot filtration test (no catalytic activity in the filtrate). XPS and TEM did not provide evidence of Pd(II) reduction and agglomeration into NPs after the reaction (suggesting strong Pd-bipy bonding), although iodine was deposited on the catalysts after the reductive elimination step.

The PSM of UiO-67-bipy NPs under similar $PdCl_2(CH_3CN)_2$ conditions resulted in the incorporation of an average number of 4.5 $PdCl_2$ per cage, which remained the same after 7 days in MeOH.[67] FTIR suggested a decrease C-N/C=N stretching frequency in accordance with the metalation of such sites. The Suzuki-Miyaura coupling between 4-bromoanisole and phenylboronic acid in a water-methanol mixture at 80 ºC using Na_2CO_3 as a base and 0.01 mol% Pd on the MOF achieved >90% yield after 12 h (79% yield after 4 h), corresponding to a TON: 9040 and TOF: 1970 h^{-1}. The material maintained its catalytic activity after 3 reaction

runs, with some leaching of Pd (5-10% of the total Pd) but not enough to catalyse the reaction by the filtrate.

The same preparation resulted in a UiO-67-bipy-Pd with 5.9 wt% Pd in the form of well-dispersed Pd(II) and characterized by series of techniques including ICP, EDX and XPS. The redshift of the C=N bonds in the FTIR spectra indicated coordination of the Pd sites at bipy embedded in the porous crystalline framework.[68] Those solids (1 mol% Pd) were highly active in the Suzuki-Miyaura coupling between chlorobenzene and phenylboronic acid at room temperature in a mixture of water-ethanol using cesium carbonate as a base, resulting in 95% yield (TON: 95) after 11 h, while <90% was obtained with other homogeneous catalysts. The yield was maintained after 5 cycles, with no observation of Pd NPs by TEM, or change in the Pd(II) oxidation state by XPS. Similar crystallinity and surface area of ca. 1400 m^2g^{-1} were found for the fresh and spent catalysts, with only 0.2 ppm Pd leached to the solution.

In another precedent, the same UiO-67-bipy-Pd MOF was directly prepared starting from the metallated bipy-Pd (using the same Pd precursor), in contrast to the PSM approach.[69] The Pd loading (1.1 wt%) was very close to the theoretical amount (1.2 wt%) for the 4 wt.% of bipy linker incorporated in the MOF. The framework was highly crystalline and porous (2000 $m^2\,g^{-1}$) as confirmed by XRD and N_2-physisoroption studied, while the $PdCl_2$ were in the form of molecular discrete sites coordinated to the N-of the pyridyl sites with oxidation state +2 as supported by from TEM, XPS and EDX analysis. The MOF was catalytically active (0.46 mol% Pd) in the Heck coupling between 4-choloroacetophenone and styrene in DMF at 100 ºC for 24 h, using K_2CO_3 and tetrabutylammonium bromide (TBAB). The use of the MOF exhibited higher activity (99 % yield, TON: 215) compared to the metallated linker (49 % yield, TON: 106) or homogeneous $PdCl_2(CH_3CN)$ catalyst (34 % yield, TON: 74). This was attributed to the better site-isolation of Pd within the MOF framework, with strong Pd-bipy bonding that avoids its aggregation and increase the lifetime of the active sites. In fact, a very low leaching of Pd was detected after a hot filtration test (ca. 46 ppb or <0.01 mol% Pd or <0.1wt. of the total Pd), which is insufficient to catalyse the coupling. The structure of the MOF and oxidation state of Pd was maintained after recycling in 5 runs. The Pd-MOF was also active in the Suzuki-Miyaura coupling between aryl chlorides and phenylboronic acid at 100 ºC for 24 h in DMF/EtOH using KOH as a base resulting in >90% yield (TON: >200).

UiO-67 and MOF-253 containing bipy linkers were used as anchoring sites for the incorporation of $Pd(OAc)_2$ at RT in acetone (ca. 8 wt.%Pd). These solids were robust to withstand the PSM conditions as confirmed by powder XRD.[70] The Pd(II)-incorporated MOFs were evaluated as catalysts (2.5 mol%) in the coupling between phenylboronic acid with 3-methylcyclohex-2-en-1-one (Scheme 6) at 100 ºC for 16 h observing 99% yield (TON: 40) for both materials. Interestingly, the Pd-containing UiO-67 without bipy sites did not promote the reaction at all, highlighting the key role of the bipy-Pd sites. Although the powder XRD of the spent Pd-MOF-253 material is similar to the fresh one, the amount of Pd leached was <1% of the total Pd loading. However, there was a decrease in the activity upon subsequent recycling eight times. Unfortunately, no information about the oxidation state of Pd after and before the reaction was provided, missing the possibility of Pd reduction and aggregation during the reaction.

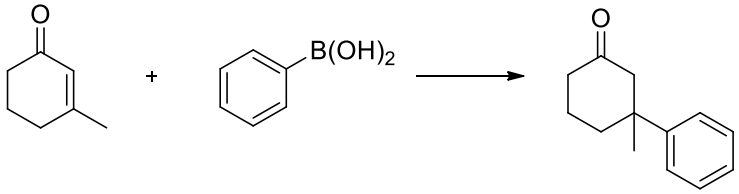

Scheme 6. C-C coupling of phenylboronic acid with 3-methylcyclohex-2-en-1-one.

In another precedent, PSM of Zr-MOF with $PdCl_2(CH_3CN)_2$ was performed at the bipyridine sites of a Zr-MOF made from two nonplanar dihydroanthracene-based tetratopic linkers, achieving a Pd loading of 1.8 wt% (almost half of the 3.2 wt% theoretical value of all the bipyridyl groups attached Pd). The successful loading of Pd(II) was reflected in the decrease of BET surface area from 1150 to 840 $m^2\,g^{-1}$.[71] The XRD pattern of the MOF was maintained, as well as the +2 oxidation state of the well-dispersed Pd(II) as confirmed by XPS and TEM-EDS mapping. The MOF catalyst (1 mol% Pd) was active in the Heck coupling between iodobenzene and ethyl acrylate at 100 ºC using TEA as a base and DMF as the solvent (100 % yield, TON: 100). The leaching of Pd was <0.1% of the total Pd and the yields were maintained after 5 reaction cycles, with no damage to the crystalline structure of the MOF.

The azobenzene linker in PCN-160 Zr-MOF was metallated with $PdCl_2$ in DMF at room temperature to obtain single Pd atoms coordinated to 1/6 of the linkers (ca. 20% Pd:Zr atomic ratio), according to Pd/Zr ratios obtained by ICP. Furthermore, XPS and ^{1}H-NMR proved that the single molecular Pd(II) species were cyclometalated palladium complexes (see Figure 4).[72] The solid was employed as a catalyst (0.8 mol% Pd) in the Suzuki-Miyaura coupling of bromobenzene with phenylboronic acid at 90 ºC in toluene, using K_2CO_3 as a base. The product yield was 95% with a TON value of 119 after 12 h which is similar to the yield obtained with a mixture of homogeneous $PdCl_2$ catalyst and the azobenzene dicarboxylate linker (90%). However, the Pd-MOF could be recovered and reused in 5 reaction runs with yields >90%, maintaining the Pd:Zr atomic ratio (15.7 vs. 15.3%) and the hot filtration test indicated no leaching of active sites. Also, the structural integrity of the PCN-160 was also retained as proved by XRD, SEM and XPS. The material was employed under continuous flow conditions (25 mg packed column) using MeOH as solvent, with a flow rate of 0.05 $mL\cdot min^{-1}$ obtaining 85% yield (TOF: 14 h^{-1}) with a final TON of 168. The decrease in yield after 12 h of flow reaction was due to the reduction of the Pd(II) single sites to Pd(0) aggregates according to XPS, although the framework integrity was maintained as confirmed by XRD and SEM analysis.

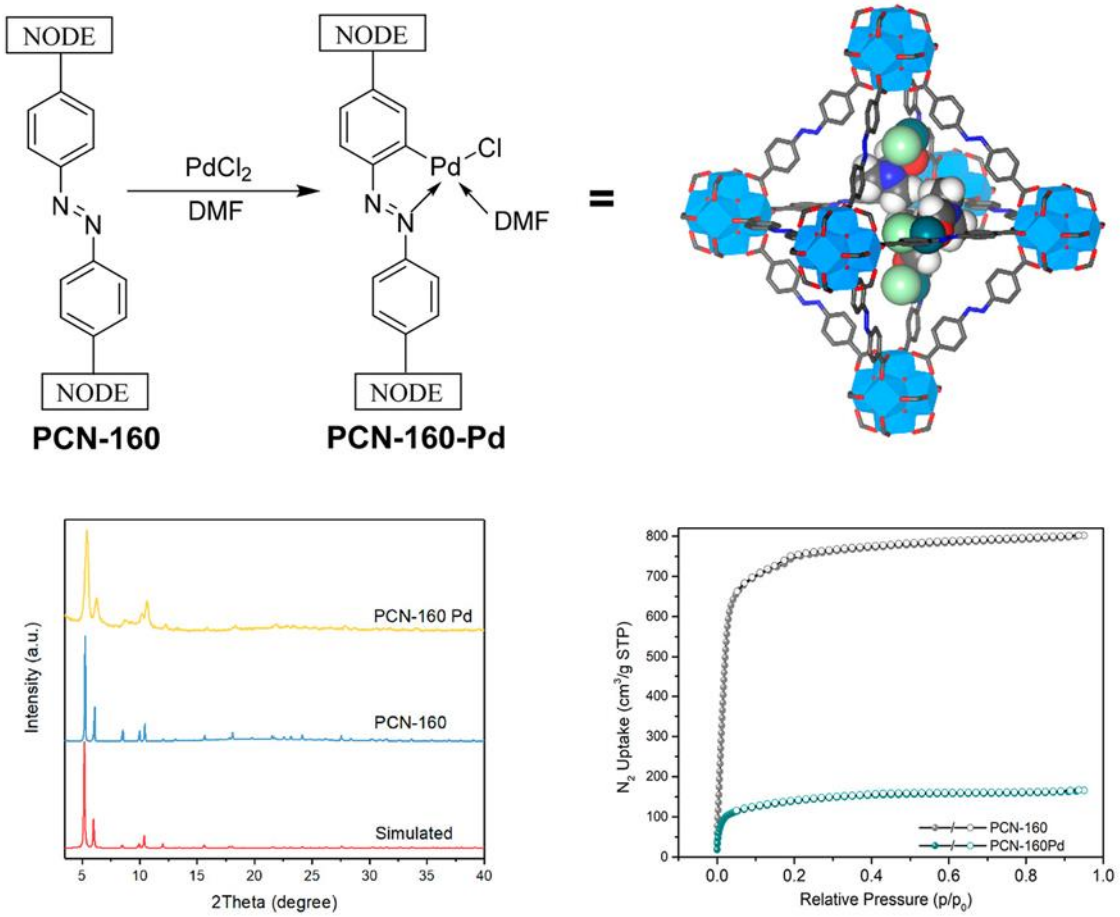

Figure 4. (a) Preparation of the PCN-160-Pd through postsynthetic metalation. (b) PXRD of PCN-160-Pd before and after metalation. (c) N_2 adsorption isotherm before and after metalation. Reproduced with permission of ref.[72] Copyright 2021 American Chemical Society.

Tripyridine groups were incorporated in an Hosmium-MOF, which was submitted to PSM with $PdCl_2(CH_3CN)_2$.[73] The resulting material maintained its structure as evidenced from XRD and incorporated 2.5 wt% Pd in the uncoordinated polypyridine groups (as the Pd-N peaks in the IR spectra indicated) was available as $PdCl_2$ (according to XPS). The Heck coupling between methylacrylate and iodobenzene using K_2CO_3 in DMF at 100 ºC for 24 h resulted in quantitative yield (100 %) with Pd-MOF (0.4 mol% Pd, TON: 248), in contrast with the 89% yield (TON: 222) for the $PdCl_2(CH_3CN)_2$ homogeneous catalyst. No reaction was observed with the filtrate (86 ppb of Pd) from a hot filtration test. Similar conditions were employed for the Suzuki-Miyaura reaction between phenylboronic acid and iodobenzene using KOH as a base, obtaining also quantitative yield after 1 h. For both reactions, the solid was active for five runs without decrease in yields or crystallinity of the MOF, and only a few Pd NPs were found in the TEM analysis of the spent catalyst.

The functionalization of UiO-66-NH_2 with biguanidine moieties allowed the grafting of K_2PdCl_4 to the -NH_2 groups under aqueous room temperature conditions (Figure 5).[74] The XRD pattern was similar before and after the metalation, while the BET surface area decreased from 831 to 629 $m^2\,g^{-1}$. The catalytic activity of the Pd-MOF (0.1 mol% Pd) was 98% yield in 10 min (TON: 980, TOF: 5880 h^{-1}) in the Suzuki-Miyaura coupling between iodobenzene and phenylboronic acid at 50 ºC in a water-ethanol mixture using K_2CO_3 as a

base. The yield was decreased to 87% after nine reaction runs, however, the crystallinity of the reused material is maintained.

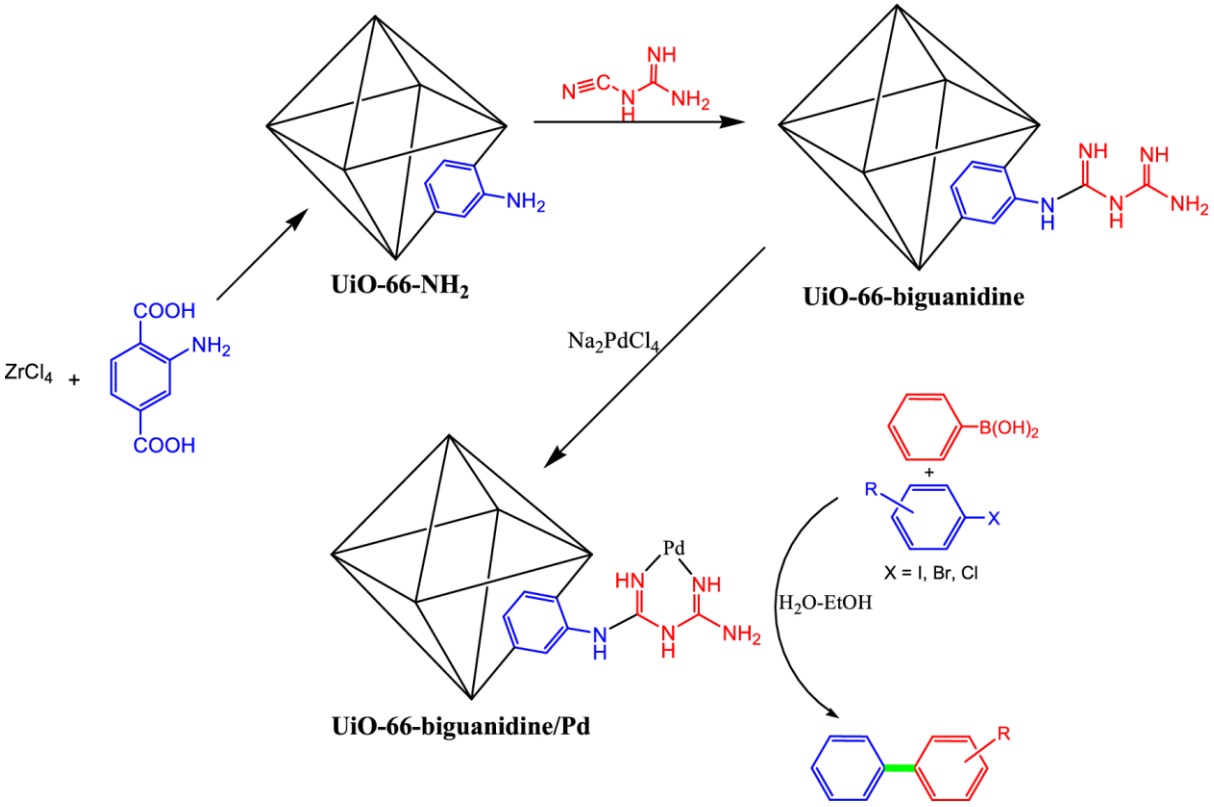

Figure 5. Sequential synthesis of UiO-66-biguanidine/Pd nanocomposite catalyst towards the Suzuki–Miyaura coupling reaction. Reproduced with permission of reference X. Copyright 2021. Springer nature.

3.2 Pd at Schiff base sites

An amino-containing La-MOF was subjected to PSM with pyridine-2-carboxaldehyde to form a Schiff base for a subsequent anchoring of $PdCl_2$ in ethanol at room temperature resulting in a 0.87 wt% Pd loading.[75] XPS indicated presence of Pd atoms in +2 oxidation state. The MOF as used as a catalyst (0.07 mol%) in the Suzuki-Miyaura coupling of iodobenzene with phenylboronic acid in ethanol at 80 ºC for 10 h using K_2CO_3 as the base, achieving 99% yield (TON: 1414). Under similar conditions, $PdCl_2$ gave 56 % yield (TON: 800). The material was recycled twelve times with yield >90 %, however minimum leaching was observed (negligible activity of the supernatant according to hot filtration test). On the other hand, the crystallinity and oxidation state was retained during the reusability tests. Interestingly, this solid was highly efficient to promote the coupling of bromobenzene and phenylboronic acid with a TON of 21443 and a TOF of 42885 h^{-1}, superior to other heterogeneous previous catalysts. This superior activity was attributed to the participation of the La nodes and organic linkers in the reductive elimination step.

Pd(II) sites (0.78 wt% Pd) were anchored in the Cu-BDC by a Schiff base PSM strategy (see Figure 6), using the unsaturated copper sites at the nodes to graft the pyridine containing imino ligand.[76] The removal of pyridine and anchoring of the hydroxyl-containing pyridine ligand was proved by FT-IR studies by monitoring the disappearance of the DMF signal and appearance of the hydroxyl signal. The XRD pattern of the Pd-modified MOF was similar to the original Cu-BDC material, with minor shifts in the main peak towards small

angles and changes in Bragg intensities, associated to the expanding of the cell due to the occupation of the void space by the Pd-containing ligand. The catalytic activity of 0.2 mol% Pd containing MOF in the Suzuki-Miyaura coupling between bromobenzene and phenylboronic acid resulted in 98% yield (TON: 490) in a DMF/water mixture using K_2CO_3 as a base at 80 ºC. The solid maintained its activity over six reaction runs.

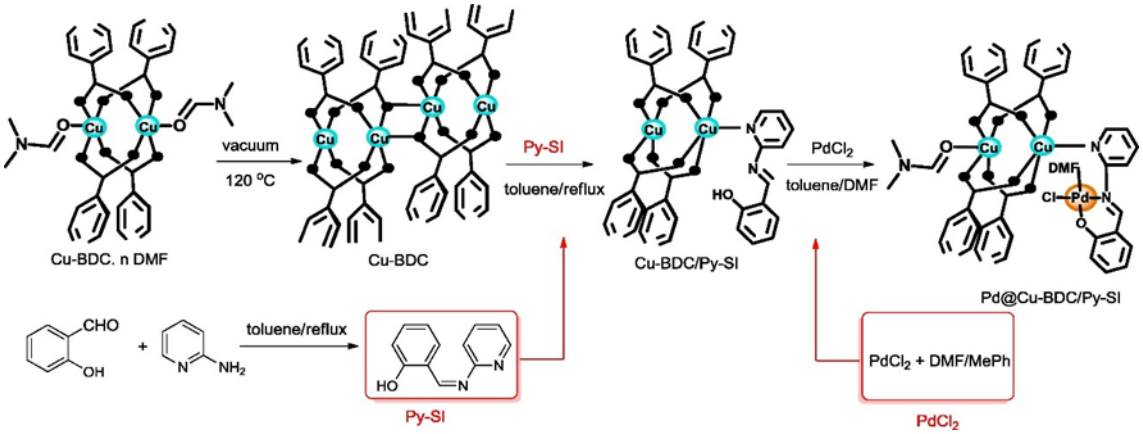

Figure 6. Functionalization of Cu-BDC with palladium complexes. Reproduced with permission of ref.[76] Copyright 2016 Elsevier.

A Zn-MOF was submitted to PSM with salicylaldehyde through the reaction of the amino group at the linker with the aldehyde group from the salicylaldehyde.[77] Two subsequent PS metalation of the salen groups (with $PdCl_2$) and Zn nodes (being exchanged by Cu) did not affect the framework structure and achieving a homogeneous distribution of Pd and Cu all over the crystal (according to EDX mapping) with some Pd(0) at the framework detected (the amount of Pd incorporated in the MOF according to this technique was 5 wt%). This technique, together with the IR bands of the imino groups observed, indicated the square planar coordination of Pd(II) bonded to one chlorine, one nitrogen, one oxygen (both from the salen complex) and one oxygen from a water molecule. The activity of the PdCu-MOF (ca. 0.5 mol% Pd) was tested in the Suzuki-Miyaura coupling between bromobenzene and phenylboronic acid at 80 ºC in a water/ethanol solvent mixture using K_2CO_3 as a base. Quantitative yield (98%, TON: 208) was obtained after five reaction runs, with no Pd leaching detected. Due to the low porosity of the MOF, the catalytic activity was assumed to be at the Pd located at the surface of the crystal.

In a similar manner, the Zn-IRMOF-3 was PSM with benzaldehyde to form the imine group to chelate (together with the benzene group) the $Pd(OAc)_2$ sites (3.5 wt% Pd) in the form of an iminopalladacycle similar to that reported for PCN-160.[78] The FT-IR and XPS analyses correspond to the imino-Pd based system, with a stable crystalline and porous structure (according to XRD and N_2-physisorption). The activity of the iminoPdMOF (0.065 mol% Pd) was studied in the Suzuki-Miyaura coupling between 4-bromobenzonitrile and phenylboronic acid in ethanol/water at room temperature for 0.5 h using K_2CO_3 achieving 98 % yield (TON of 1507 and TOF of 3015 h^{-1}). Under the same conditions, the use of $Pd(OAc)_2$ only resulted in 55 % yield after 5 h (TON: 846, TOF: 170 h^{-1}), which could not be recovered and recycled due to the formation of Pd black. In contrast, the solid MOF showed good reusability in five runs without appreciable leaching (less than 0.5 wt% of the initial Pd).

The introduction of amino salicyl-like fragmented linker (defect engineering approach) in the framework of Ni-MOF-74 was achieved via coordination of the -COOH and -OH groups to the Ni-oxo clusters for further PSM with pyridine carboxaldehyde generating the Schiff base ready to coordinate Pd active sites (Figure 7).[79] The crystalline structure was preserved during the whole PSM process, and the pore size distribution suggests a modification of the pores around the defective positions involving the Schiff-base linker, which reduced the pore size after the Pd metalation. The incorporated Pd(II) sites were catalytically active (1.3 mol% Pd) in the Suzuki-Miyaura coupling between bromobenzene and phenylboronic acid at 100 ºC in toluene using K_2CO_3 as a base for 24 h. The yield of 99 % was (TON: 76) superior to $PdCl_2$ (60%, TON: 46) and the activity of the MOF maintained over five reaction cycles (as well as the MOF crystallinity), with no appreciable leaching in the hot filtration test.

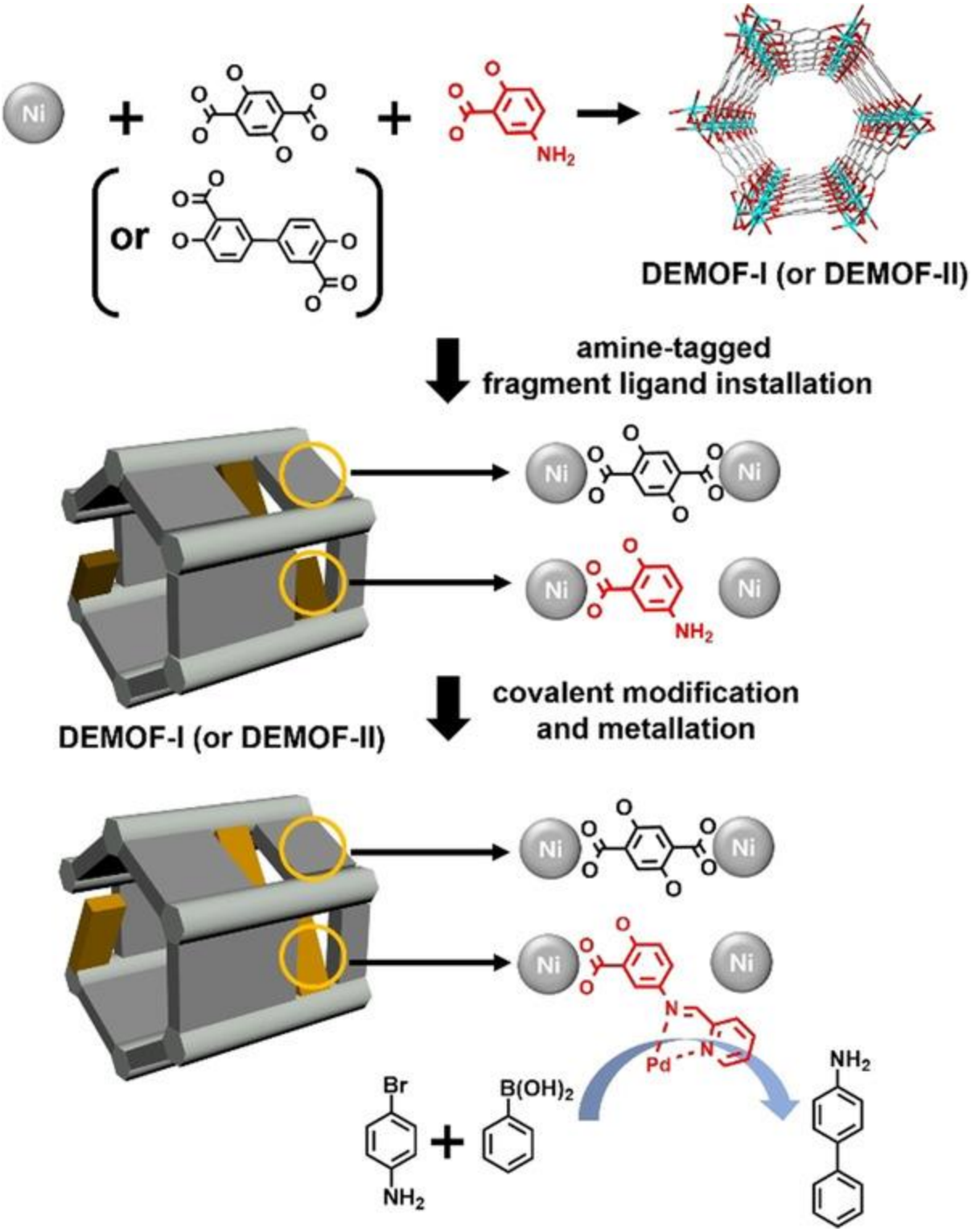

Figure 7. Covalent modification and metalation of DEMOF-I (or DEMOF-II) prepared by a de novo solvothermal reaction by employing the mixed ligands DOBDC (or DODPDC) and an amine-tagged fragment, and the Suzuki–Miyaura cross-coupling reaction using Pd-incorporated DEMOF-I as a heterogeneous catalyst. Reproduced with permission of reference X. Copyright 2021 (Wiley).

Similar pyridylimine groups were incorporated in the linker of a Sr-MOF with free amino groups at the benzene ring of the linker, which acted as a Schiff base coordinating Pd

(up to 11.11%) in a square planar *cis* geometry.[80] This bonding was confirmed by UV-Vis, FT-IR and the decrease in BET surface area from 2052 to 1636 $m^2 g^{-1}$ after the PSM steps. The activity of the MOF (0.1 mol% Pd) was tested in the Suzuki-Miyaura coupling between bromobenzene and phenylboronic acid in a water/ethanol mixture at 80 ºC for 1-2 h, in the presence of K_2CO_3 as a base by observing 99% yield (TON: 990, TOF: 958 h^{-1}).The activity, crystallinity, composition and porosity was retained for five reaction cycles.

3.3 Pd at N-heterocyclic carbenes

The benzene ring of the linker of MIL-101 was functionalized with an imidazolium chloride, for the subsequent generation of the N-heterocyclic carbene (NHC) after treatment with $Pd(OAc)_2$ in ethanol (Figure 8) (loading 1.26 $mmol \cdot g^{-1}$ Pd).[81] Interestingly, XPS and TEM analyses of the as-prepared material indicated the presence of Pd NPs. The Pd-MOF was tested as a catalyst (0.8 mol%) in the Mizoroki-Heck coupling between bromobenzene and styrene in DMF at 110 ºC, using K_2CO_3 as a base, obtaining 96% yield after 6 h (TON: 160). In contrast, only 65% yield (TON: 108) was obtained with $Pd(OAc)_2$ and PPh_3 under similar conditions. The MOF was recycled five times with only minor decrease in yield (<10%) and Pd leaching (6.8 ppm or less than 4% of the Pd). Under similar conditions (1 mol% Pd), the MOF promotes the Sonogashira coupling between phenylacetylene and bromobenzene resulting in 91% yield (TON: 91) and maintained its activity up to five recycles (only 4% Pd and 3% Cr leached).

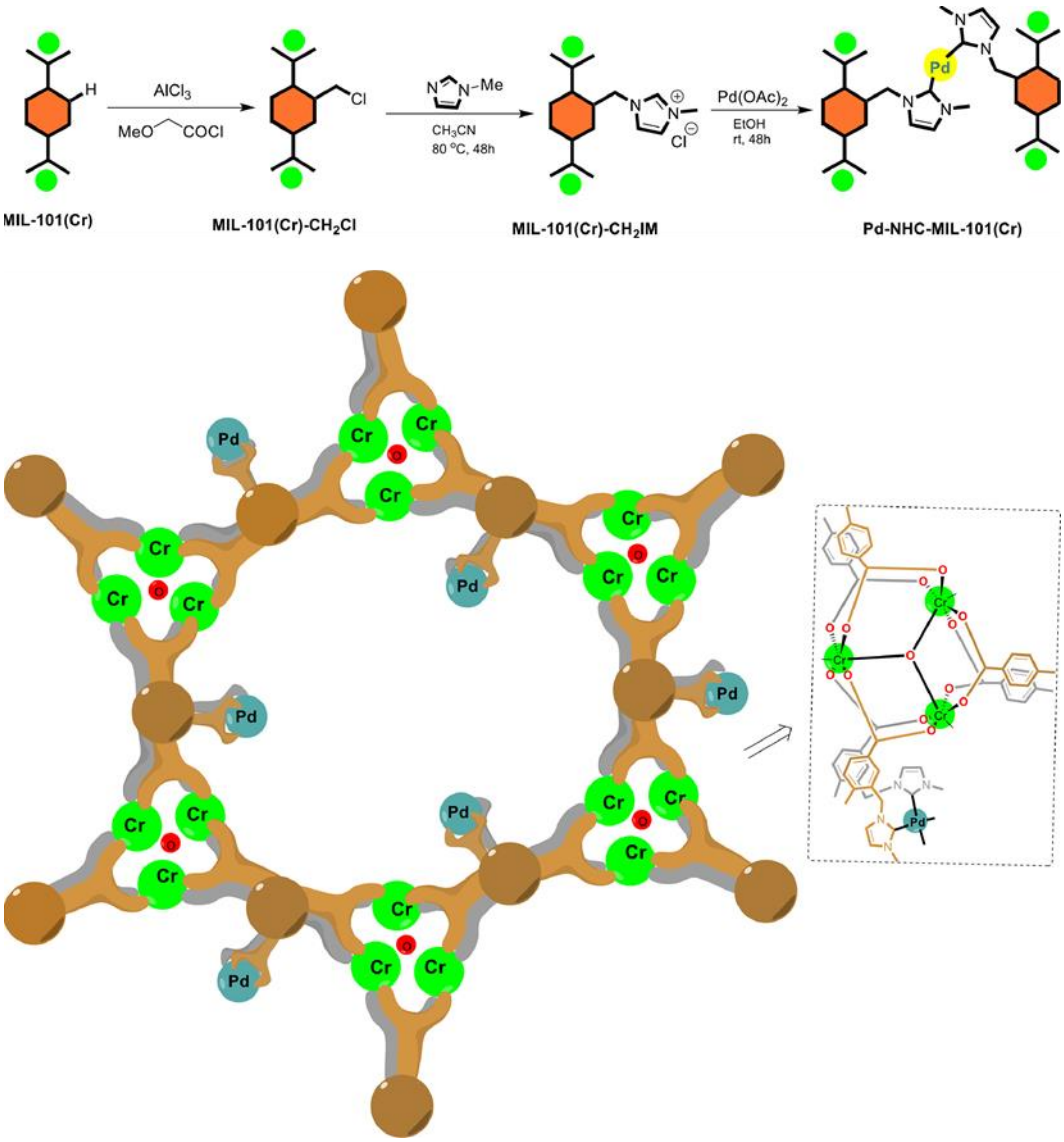

Figure 8. Synthetic route for the preparation of Pd-NHC-MIL-101(Cr) catalyst and its structure. Adapted with permission of ref.[81] Copyright 2021 Elsevier.

A triazine functionalized MIL-101-NH_2 was PSM with imidazolium chloride and $Pd(OAc)_2$ in DMSO at 100 ºC, decreasing the pore size from 3.8 to 3.4 nm due to the presence of the Pd-NHC in the MOF pores.[82] The Pd was half in the form of Pd(II) and Pd(0), according to XPS, but no Pd clusters were observed by TEM, indicating the isolation of Pd(0) at the NHC sites. The activity of the MOF was evaluated in the Suzuki-Miyaura coupling between bromobenzene and phenylboronic acid at 60 ºC in DMF/water, using K_2CO_3 for 0.5 h, was a 100% yield of product with a TOF of 625 h^{-1} (TON: 1250). The MOF was reused 15 times with only 0.06 $mmol_{Pd} \cdot g^{-1}$ leached out, resulting in <10% increase in the conversion after a hot filtration test.

A double imidazolium bromide was introduced in the biphenyl linker of UiO-67, which after reaction with $Pd(OAc)_2$ resulted in the N-heterocyclic dicarbene (NHDC), characterized by NMR and MS.[83] The UiO-67-Pd-NHDC MOF was obtained by directly reacting this linker with zirconium chloride and standard 4,4'-biphenyldicarboxylate linker under solvothermal conditions (Figure 9). The XRD confirmed the formation of pristine UiO-67, with a porous

structure having less BET surface area (1540 *vs*. 2113 $m^2 g^{-1}$) and the Pd loading was 1.0 wt%, according to ICP analysis. Palladium oxidation state was in the divalent state as confirmed by XPS. The MOF (0.5 mol% Pd) was tested in the Heck coupling between iodobenzene and ethylacrylate using TEA and TBAB at 120 ºC in DMF, resulting in a TON and a TOF of 196 and 196 h^{-1} respectively. No changes in the activity, crystallinity, Pd content and oxidation state were observed upon recycling in five runs, due to the strong covalent double N-heterocyclic bond of Pd.

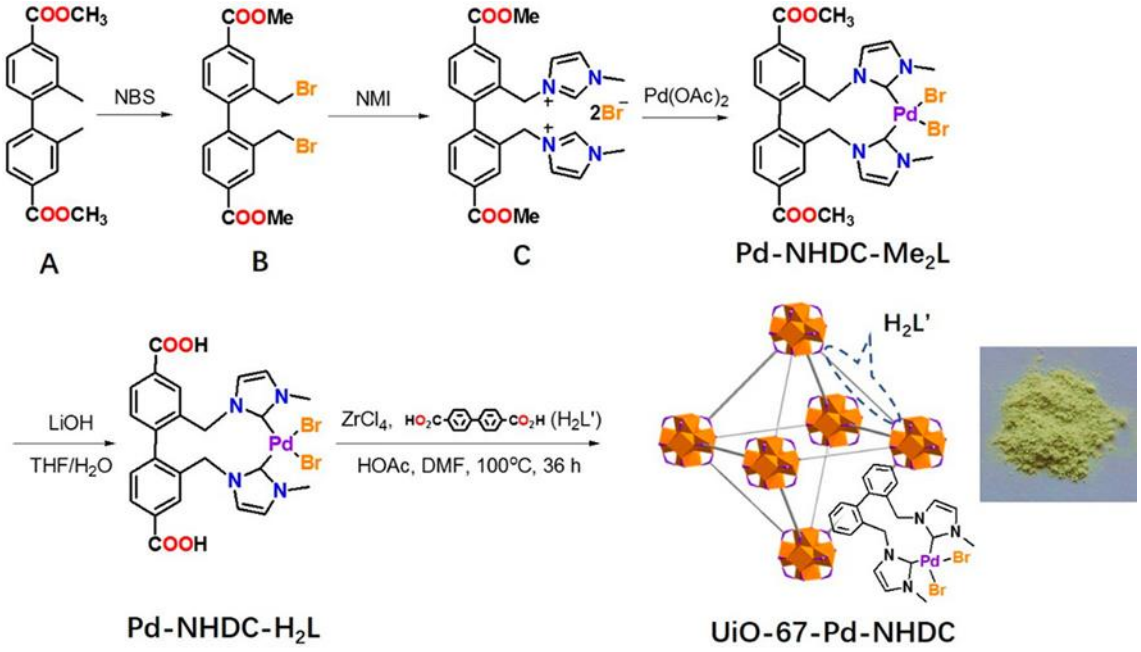

Figure 9. Synthesis of Pd-NHDC-H_2L Ligand and UiO-67-Pd-NHDC MOF. Reproduced with permission of ref.[83] Copyright 2018 American Chemical Society.

A solvothermal reaction between 1,3-bis(4-carboxyphenyl)imidazolium chloride and zinc nitrate resulted in the azolium-containing MOF. This solid was treated with Pd(II) salts to anchor these Pd(II) ions through NHC sites.[84] The activity of azolium-containing MOF-Pd was tested in the Sonogashira coupling between 2-bromopyridine and 4-methoxyphenylacetylene in DMF at 100 ºC using cesium carbonate as a base to obtain 84% yield. This solid showed wide substrate scope in moderate to higher yield. The catalyst activity was not altered up to four cycles. Powder XRD patterns of the used solid was identical to the fresh solid. TEM and XPS analysis of the used showed no changes in the particle size and oxidation state, respectively.

Other MOFs employ phosphine groups at the organic linker for the grafting of Pd sites, such as the Pd-P-modified MIL-101. The catalyst (3 mol% Pd) was employed in the Suzuki coupling between 3-bromoanisole and phenylboronic acid at 90 ºC using 3 eq. of trimethylamine. The Pd(II) bonding to the P sites was proved by P K-edge XAS and 31P-MAS-NMR, which was partially preserved in the spent catalyst despite from the formation of reduced Pd nanoparticles from the decomposition of the mono-coordinated Pd-P sites. The better performance of the molecular Pd-P catalyst over Pd nanoparticles formed during the reaction was due to the higher selectivity to the coupling product with respect to hydrodehalogenation in the presence of the nanoparticles. An increase in the phosphine amount avoids the formation of Pd nanoparticles and thus increases the cross-coupling activity of the heterogeneous Pd-P-MOF catalyst.

4. Pd NPs on MOFs

The following sections will summarize the catalytic activity of Pd NPs supported over different MOFs and the catalytic activity of these MOFs is discussed in the cross coupling reactions. The existing works are categorized based on the nature of MOFs. The catalytic activity of Pd NPs encapsulated on various MOFs is also compared with homogeneous counterparts as well as Pd NPs supported over other solids to illustrate the efficiency of MOFs as supports for the stabilization of NPs.

Pd NPs with 2-5 nm were synthesised within the pores of MOF-5 by employing metal-organic chemical vapour deposition method and the resulting solid (Pd@MOF-5) was tested in the Suzuki-Miyaura coupling between phenylboronic acid and bromobenzene in DMF with K_2CO_3 as the base at 90 ^oC for 20 h.[85] The maximum conversion of 81% was observed with 4.2% Pd, however, the activity decreased to 21% after 4 runs. This loss in the activity was due to the collapse of the crystal structure of MOF-5 as confirmed by powder XRD.

In one of the earlier contributions, Pd NPs were supported on MOF-5 (Pd/MOF-5) by using a chemical method at room temperature and its catalytic performance was tested in the Sonogashira coupling reaction.[86] The uniformly dispersed Pd NPs size over MOF-5 was 3-6 nm from TEM analysis. Out of the different experimental conditions screened, the use of Pd/MOF-5 as heterogeneous catalysts facilely coupled iodobenzene with phenylacetylene using K_3PO_4 as a base in methanol at 80 ^oC after 3 h under nitrogen atmosphere to achieve 98% yield. Furthermore, Pd/MOF-5 was also effectively used to couple wide ranges of substrates with high yields under these conditions. Although the activity of Pd/MOF-5 was retained up to two cycles, the activity significantly dropped after 5 runs to 49% yield. Although the leaching of Pd was ruled out for the catalyst deactivation, the XPS studies of the recycled catalyst showed the existence of Pd(II) which was absent in the fresh solid catalyst. On the other hand, TEM images also revealed the presence of agglomerated Pd NPs in the reused solid.

A novel Au/Pd-functionalized over UiO-66-NH_2 was prepared (Figure 10; Au/Pd@UiO-66-NH_2) and its catalytic activity was tested in the Suzuki-Miyaura coupling reaction under visible light irradiation.[87] Further, TEM and HRTEM analyses proved the existence of Au/Pd bimetallic alloy NPs with an average size of 6.45 nm. Among the various experimental conditions examined, (1:2) Au/Pd@UiO-66-NH_2 exhibited >99% conversion with the TOF value of 426 h^{-1} in EtOH/H_2O medium using K_2CO_3 as a base after 1 h. The photostability of Au/Pd@UiO-66-NH_2 was tested and observed identical activity for three consecutive cycles without much change in the particle size morphology.

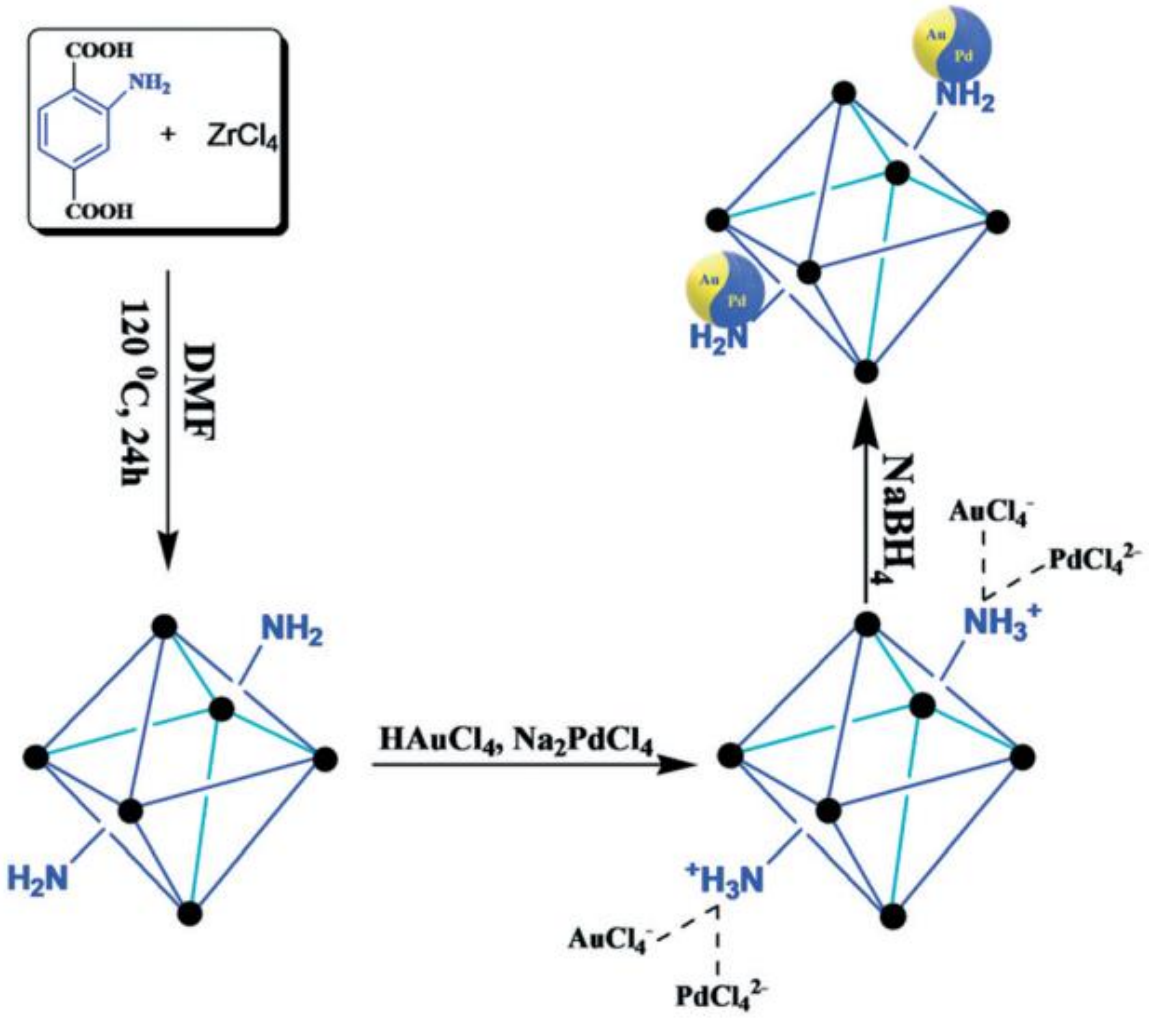

Figure 10. Schematic of the synthesized Au/Pd@UiO-66-NH_2 composite. Reproduced with permission from ref.[87] Copyright Royal Society of Chemistry 2019.

Recently, a bifunctional heterogeneous catalyst was prepared consisting of Pd NPs and chiral proline on NH_2-UiO-66 solid to obtain Pd@NH_2-UiO-66(pro)-1 solid catalyst (Figure 11).[88] Pd NPs were encapsulated inside the framework of NH_2-UiO-66 by employing the "bottle-around-ship" method, while chiral proline was decorated to the zirconium nodes and the organic linkers via coordination and PSM, respectively. The catalytic activity of Pd@NH_2-UiO-66(pro)-1 was checked in the Suzuki-Miyaura coupling of 4-bromobenzaldehyde and phenylboronic acid using K_2CO_3 as a base in EtOH/H_2O (1:1) mixture at 80 ^oC after 10 min with quantitative yield of 4-formylbiphenyl. On the other hand, Pd@NH_2-UiO-66(pro)-1 solid was reusable for four cycles with no decay in the yield. Furthermore, powder XRD pattern of the reused solid was intact with no collapse in the crystalline pattern.

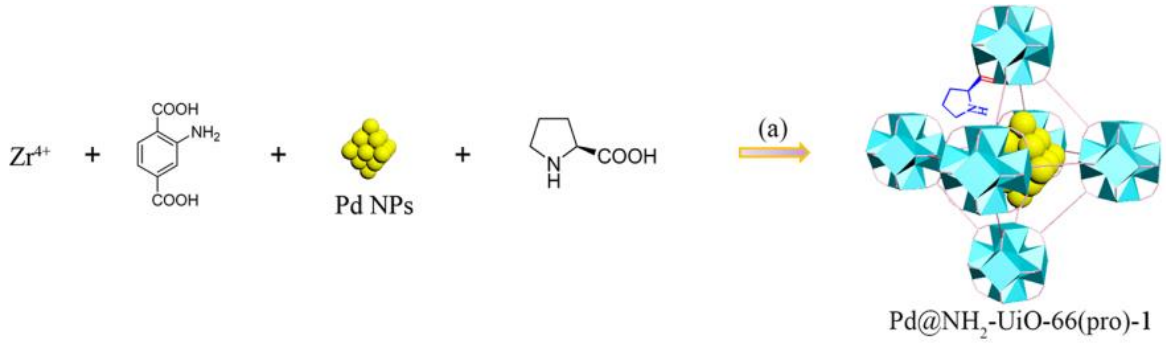

Figure 11. Synthetic of Pd@NH_2-UiO-66(pro)-1 by solvothermal method. Reproduced with permission of ref.[88] Copyright 2020 American Chemical Society.

Pd NPs was deposited over glyoxal condensed with UiO-66-NH_2 and the activity of the resulting solid UiO-66-NH_2-GI@Pd (Figure 12) was examined in the Sonogashira coupling reaction.[89] The average particle size of Pd NPs was around 10 nm. The activity of UiO-66-NH_2-GI@Pd was tested in the coupling between iodobenzene and phenylacetylene using K_2CO_3 as base in water/ethanol mixture at 70 ^oC. The desired product yield was 95% while the TON and TOF values were 1900 and 3800 h^{-1}, respectively. This catalyst exhibited wide substrate scope thus indicating its efficiency in achieving library of products under mild reaction conditions. Although the catalyst was reusable four cycles, the time to maintain its activity is gradually increased. Further, ICP analysis revealed partial leaching of Pd NPs under these conditions.

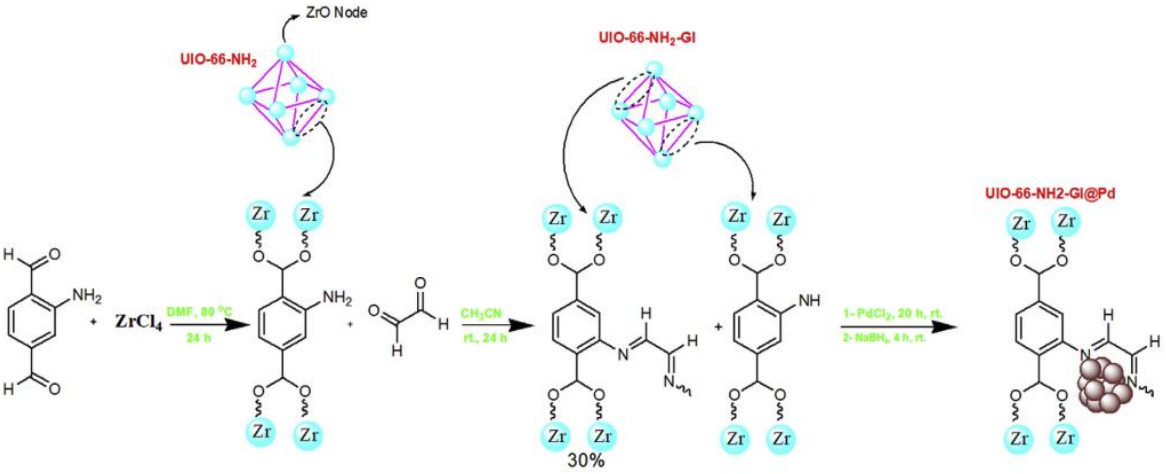

Figure 12. PSM procedure for UiO-66-NH_2. Reproduced with permission of ref.[89] Copyright 2020 Elsevier.

Pd NPs (2 ± 0.3 nm) were encapsulated within the pores of in a series of isoreticular mixed-linker MOFs and the resulting MOF-Pd NPs (Figure 13) were reported as heterogeneous catalysts for the Suzuki-Miyaura coupling reaction between phenylboronic acid and iodobenzene.[90] Notably, m-6,6′-Me_2bpy-MOF-Pd solid showed a remarkable activity compared to non-functionalized m-bpy-MOF-Pd and m-4,4′-Me_2bpy-MOF-Pd using K_2CO_3 as a base in toluene at 85 ^oC (Figure 14). This study is an illustrative example to demonstrate the influence of stereoelectronic properties of linker. The solid m-6,6′-Me_2bpyMOF-Pd catalyst was reused for three consecutive cycles with no decrease in the yield of biphenyl. Although powder XRD of the reused solid shoed identical XRD pattern with

the fresh solid, TEM images of the used m-6,6′-Me_2bpy-MOF-Pd solid showed significant aggregation of Pd NPs.

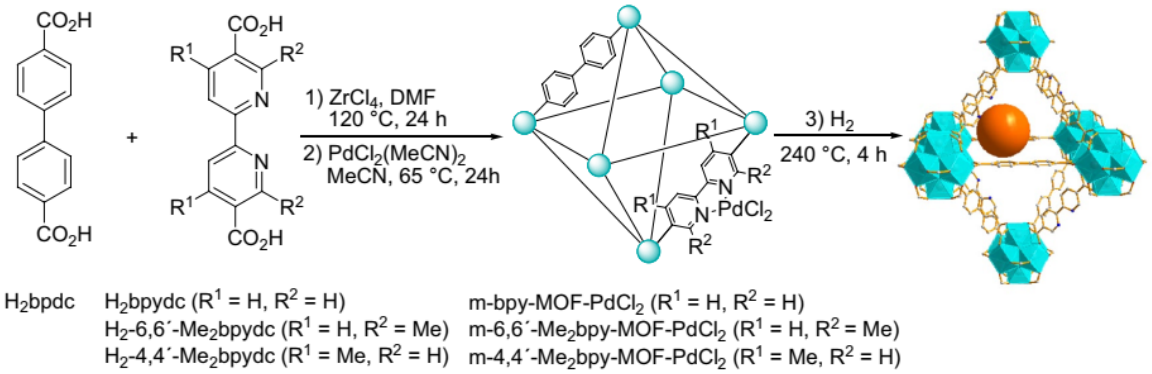

Figure 13. Schematic representation of the synthesis of Pd NPs encapsulated in isoreticular m-bpy-MOFs. Green sphere and octahedra represent Zr clusters, while orange spheres represent Pd NPs. Reproduced with permission of ref.[90] Copyright 2018 Springer.

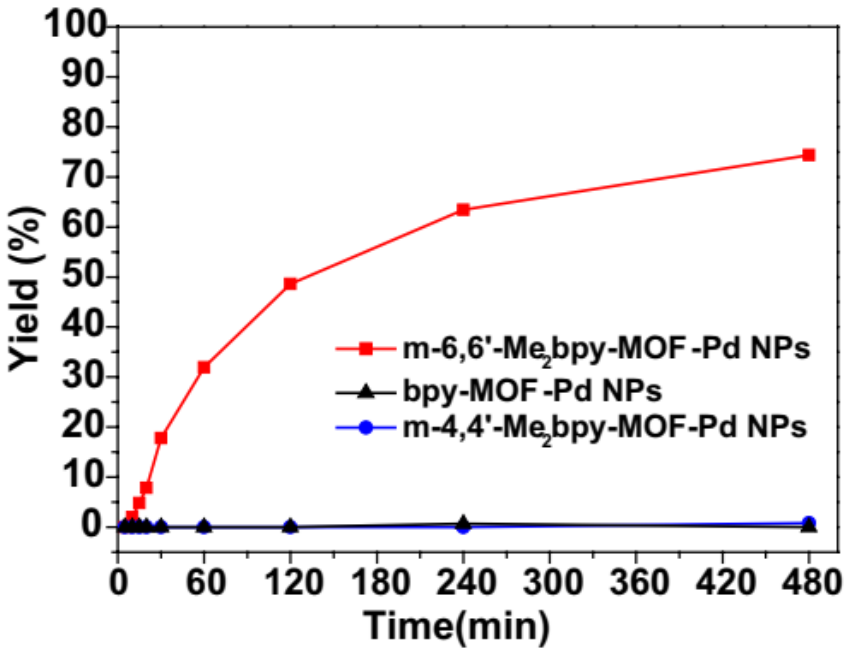

Figure 14. The catalytic difference of m-MOF-Pd in the Suzuki-Miyaura coupling reaction of iodobenzene. Reproduced with permission of ref.[90] Copyright 2018 Springer.

Mixed-linker MOFs (Scheme 7) based on MIL-53(Al) were synthesised and Pd NPs were supported on mixed linker MIL-53(Al) MOFs.[91] TEM analysis showed that Pd NPs are highly distributed on the outer surface of MOF with the average particle size of 3.2 nm. The catalytic performance of different solids was tested in the Heck coupling between bromobenzene and styrene using triethylamine as a base in DMF at 120 °C. Pd/MIL-53(Al) showed 26% yield (TOF: 87 h^{-1}) under these conditions. On the other hand, the activity was gradually increased upon increasing amino-functionalized linker and then the activity decreased. For instance, the yield of the coupling product with Pd/MIL-53(Al) with 10% NH_2 was 76% (TOF: 254 h^{-1}) while it was 93% (TOF: 310 h^{-1}) and 86% (TOF: 287 h^{-1}) for Pd/MIL-

53(Al) with 50% NH_2 and Pd/MIL-53(Al) with 90% NH_2, respectively. Furthermore, the activity of Pd/MIL-53(Al)-NH_2 was 81% (TOF: 270 h^{-1}), which is lower than to Pd/MIL-53(Al) with 50% NH_2. These results prove the merit of mixed linker MOFs in providing better stabilization of Pd NPs to increase the catalytic efficiency. On the other hand, Pd/C showed only 49% yield (TOF: 164 h^{-1}) under identical conditions. Although this solid provided better activity with bromobenzene and iodobenzene, the yield was 11% with chlorobenzene. Also, the solid showed wide substrate scope in preparing series of olefin derivatives under these conditions. The catalyst was active for five cycles with no decay in its activity. Leaching test showed 0.1 ppm of Pd and TEM images of the used solid showed a slight increase of Pd NPs size to 3.4 nm.

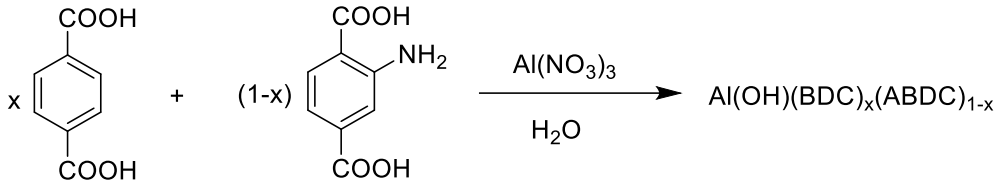

Scheme 7. Synthesis of mixed linker MOFs based on MIL-53(Al). BDC: benzene-1,4-dicarboxylate, ABDC: 2-aminobenzene-1,4-dicarboxylate.

Pd NPs were supported on the surface of Ni-MOF partially carbonized PAN [PAN(C)] by solvothermal method.[92] Ni-MOF@PAN(C) possessed highly abundant oxygen sites which are responsible for the stabilization of Pd NPs. Among the different catalytic conditions screened, Pd_1/Ni_4-MOF@PAN(C) exhibited the highest activity for the Suzuki-Miyaura coupling between iodobenzene and phenylboronic acid affording 97% conversion with K_2CO_3 as a base after 1.5 h at 80 °C (TOF:717). Although the activity of Pd_1/Ni_4-MOF@PAN(C) was relatively higher (90-95%) for the Suzuki-Miyaura coupling of phenylboronic acid with bromo-and iodoarenes, the Suzuki-Miyaura coupling of phenylboronic acid with chlorobenzene was negligible. Further, the solid maintain its activity for sic cycles with no change in the oxidation state and particle size of Pd.

A simple and green approach was designed to prepare Pd@[$Ni(H_2BDP\text{-}SO_3)_2$] (BDP-SO_3: 2,5-di(1H-pyrazol-4-yl)benzenesulfonate) possessing both Pd^{2+} and Pd NPs in a Ni(II) pyrazolate MOF (Figure 15).[93] Further, Pd NPs were in the range of 4-8 nm from TEM images. The activity of Pd@[$Ni(H_2BDP\text{-}SO_3)_2$] was tested in the Suzuki-Miyaura coupling reaction between 2-bromotoluene and phenylboronic acid using K_2CO_3 as a base in 2-propanol/water (1:1) mixture at 60 ^oC achieving 99% yield after 4 h. Under identical conditions, the use of 2-chlorotoluene resulted in no product formation even after 20 h at 100 ^oC. Reusability experiments showed a gradual decrease in the conversion from 98 to 80% for the 1st to 4th cycle, respectively. The four times used catalyst was characterized by powder XPRD and observing certain degree of MOF crystallinity loss. Further, TEM images of the used catalyst still exhibited homogeneously distributed Pd NPs with no agglomeration.

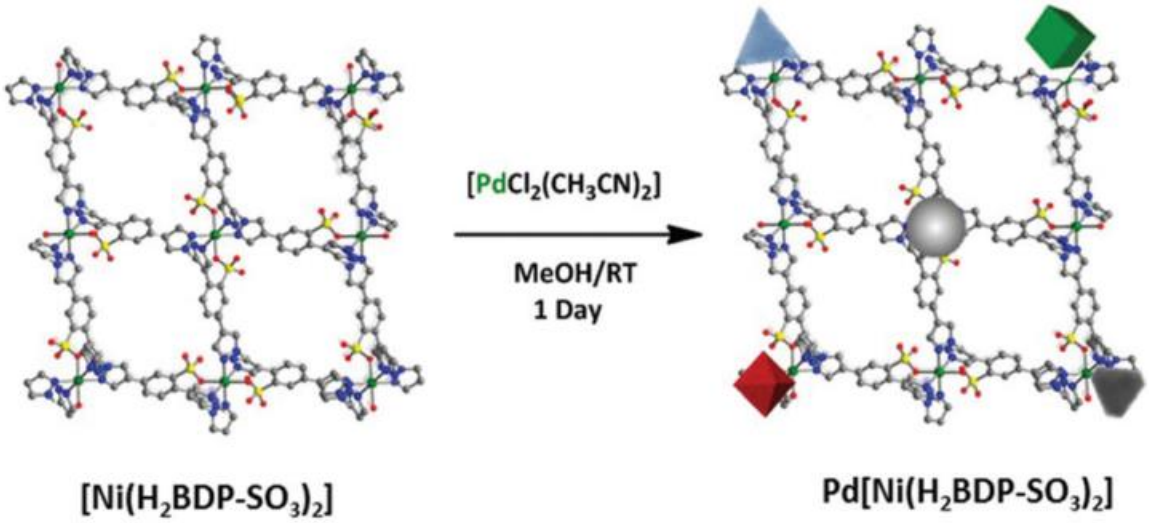

Figure 15. Green preparation of Pd@[Ni(H_2BDP-SO_3)$_2$] catalyst. Reproduced with permission of ref.[93] Copyright 2016 Royal Society of Chemistry.

Pd NPs (7 nm) were immobilized over MOF-808 to afford Pd@MOF-808 as a stable and single-site catalyst and its catalytic performance was examined in the Suzuki-Miyaura coupling reaction between 4-iodoanisole and phenylboronic acid in methanol at 40 ^{o}C using K_2CO_3 as a base.[94] Among the various experimental conditions screened, Pd@MOF-808 afforded 99% yield of the desired product under mild reaction conditions. In addition, this solid exhibited a wide substrate scope for the facile Suzuki-Miyaura coupling between aryl/heteroaryl iodides with phenylboronic acid derivatives in high yields. Reusability experiments clearly indicated that the activity of Pd@MOF-808 was mostly retained up to five cycles, but, it suddenly dropped to 49% in the sixth cycle. Spent catalyst characterization proved that the loss of activity was neither due to the leaching of Pd nor to the collapse of the crystal structure, but the surface of Pd NPs was covered by halide ions. Interestingly, the drug, fenbufen was successfully synthesised in 90% yield by Suzuki-Miyaura coupling reaction between the intermediate and the phenylboronic acid using Pd@MOF-808 as a heterogeneous solid catalyst (Scheme 8).

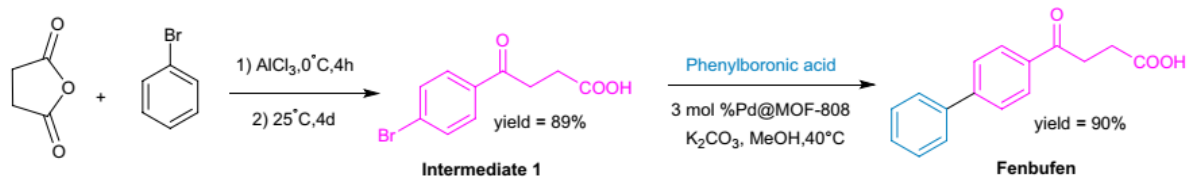

Scheme 8. Synthesis of fenbufen.

In one of the seminal contributions, Belen and co-workers have reported the immobilization of Pd NPs within the framework of MIL-101(Cr)-NH_2 to obtain Pd@MIL-101(Cr)-NH_2 with different Pd loadings. Pd NPs were uniformly distributed with the average particle size of 2.6 nm.[95] Among the various solids tested with different Pd loadings in Pd@MIL-101(Cr)-NH_2, 8wt% Pd@MIL-101(Cr)-NH_2 afforded 99% yield in the Suzuki-Miyaura coupling between bromobenzene and organoboron reagent in water using K_2CO_3 as a base at room temperature. One of the notable features of this catalyst is that it exhibited the facile Suzuki-Miyaura coupling between wide ranges of substrates leading to the desired

products in higher yields. Furthermore, the catalyst was recycled at least 10 times with no difference in its catalytic performance (Figure 16).

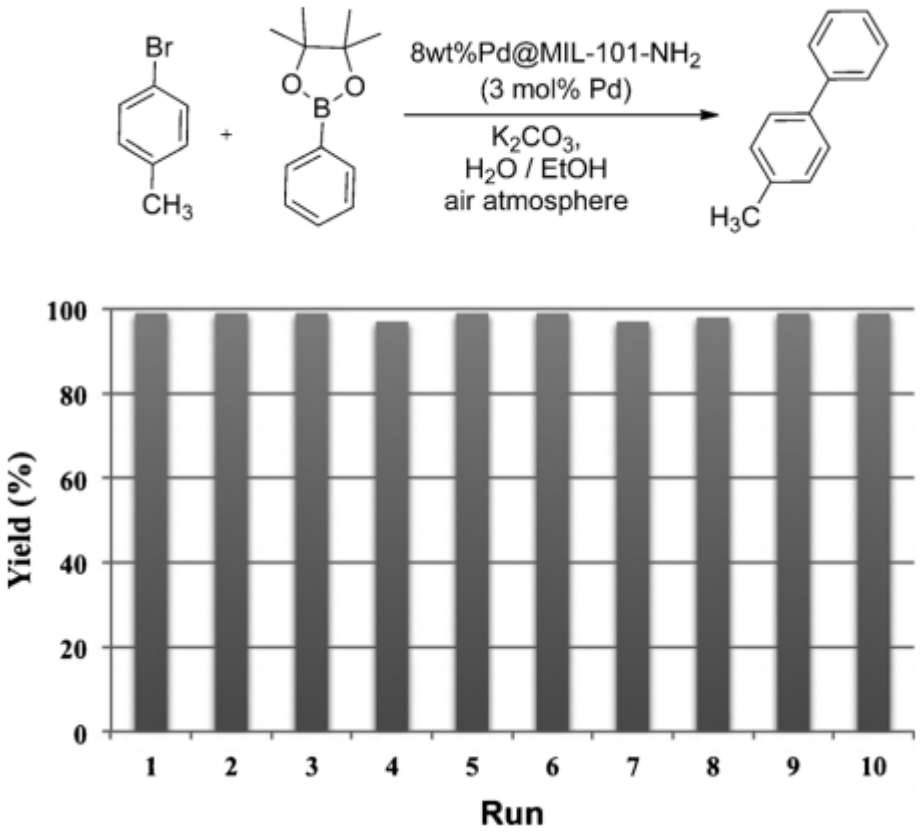

Figure 16. Recycling experiments on a 1 mmol scale; reaction time of each run: 0.5 h. Reproduced with permission of ref.[95] Copyright 2013 Wiley.

Later, the same group has reported the influence of the base in the Suzuki-Miyaura coupling reaction between 4-methylbromobenzene and 4-methylphenylboronic acid in H_2O/EtOH (1:1) at 25 ºC using Pd@MIL-101-NH_2(Cr) as solid catalyst.[96] Among the four bases (K_2CO_3, KF, Cs_2CO_3 and CsF) tested in the above Suzuki-Miyaura reaction, the use of carbonates accelerated the reaction rate by showing high yields in short reaction time compared to fluorides. On the other hand, powder XRD and N_2 sorption measurements revealed that the MOF was degraded with carbonates as base but remained crystalline and porous with the use of fluorides as bases. Furthermore, it was also noticed that the different counter cations of the base also significantly influenced the catalytic activity of the solid. Also, TEM images indicated that the Pd NPs were larger after multiple reuses using caesium as bases compared to potassium based bases (Figure 17).

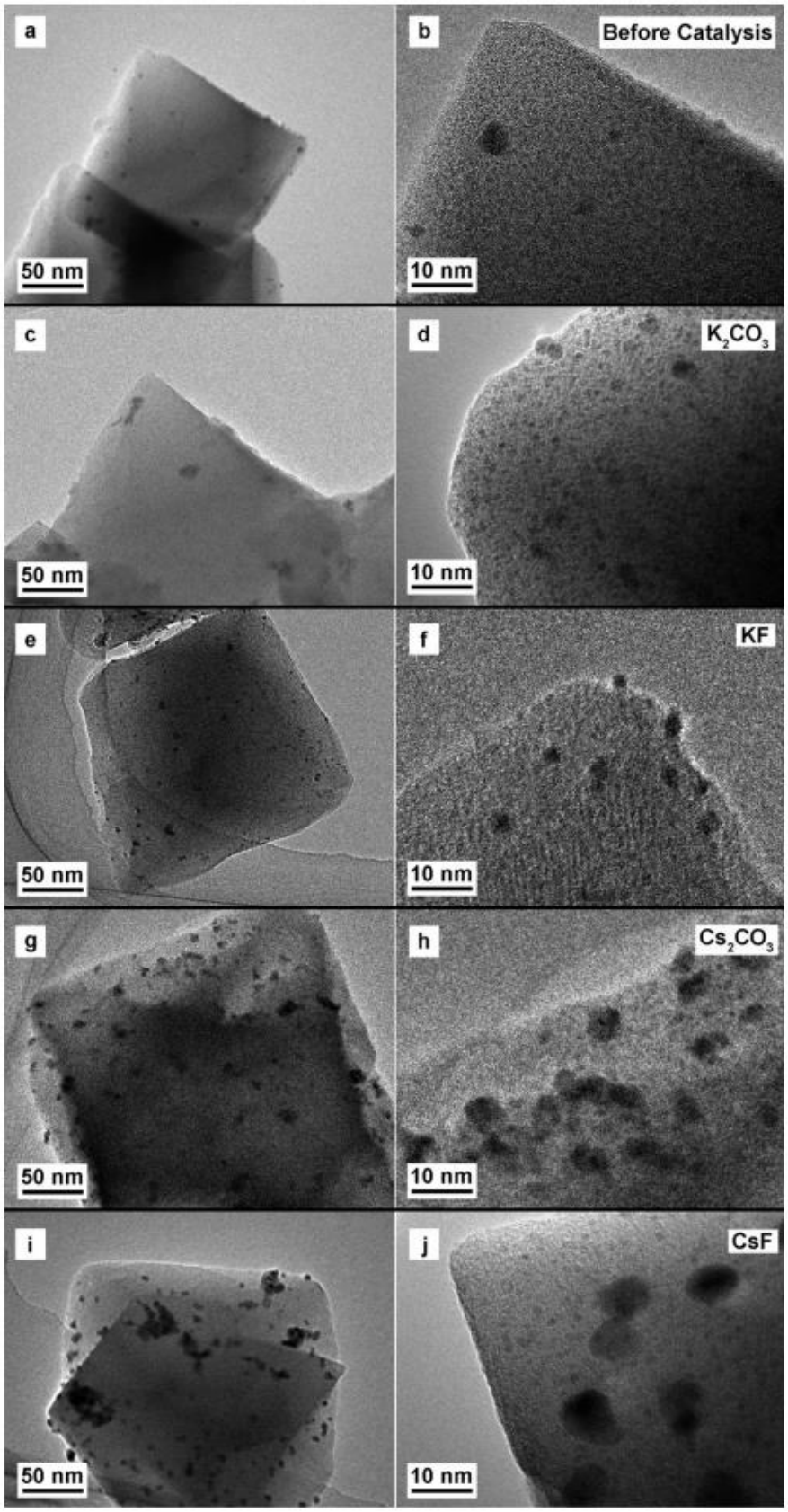
a
50 nm
b
Before Catalysis
10 nm
c
50 nm
d
K_2CO_3
10 nm
e
50 nm
f
KF
10 nm
g
50 nm
h
Cs_2CO_3
10 nm
i
50 nm
j
CsF
10 nm

Figure 17. TEM images of Pd@MIL-101-NH_2(Cr) a), b) before catalysis and after three runs of catalysis with c), d) K_2CO_3, e), f) KF, g), h) Cs_2CO_3 and i), j) CsF as base. Reproduced with permission of ref.[96] Copyright 2015 Wiley.

Importantly, Pd@MIL-101-NH_2 was packed in a micro-flow reactor and its activity was tested in the Suzuki-Miyaura coupling reaction under continuous flow conditions.[97] As shown in Scheme 9, a library of 11 isolated compounds was synthesised under flow conditions without replacing the catalyst, thus demonstrating the potential of Pd NPs embedded over MOFs for the large-scale applications. On the other hand, Pd@MIL-101-NH_2 (0.01 mol%) was employed as a heterogeneous solid catalyst for the Suzuki-Miyaura coupling reaction between 4-bromoacetopheneone (7.5 gram scale) and an equimolar of p-tolylboronic acid. The desired 4-(4'-methylphenyl) acetophenone was obtained in 99% yield after 280 min with a TON value of 10000 in high purity as evidenced from ^{1}H NMR. Later, 4-(4'-methylphenyl) acetophenone was reacted with alloxan hydrate to afford MMP inhibitor for matrix metalloproteinases involved in inflammatory diseases, in 95% yield after 3 h (Scheme 10). This process provided a relatively better approach for the synthesis of this compound compared to an earlier report by Nicolotti et al with 50% overall yield.[98]

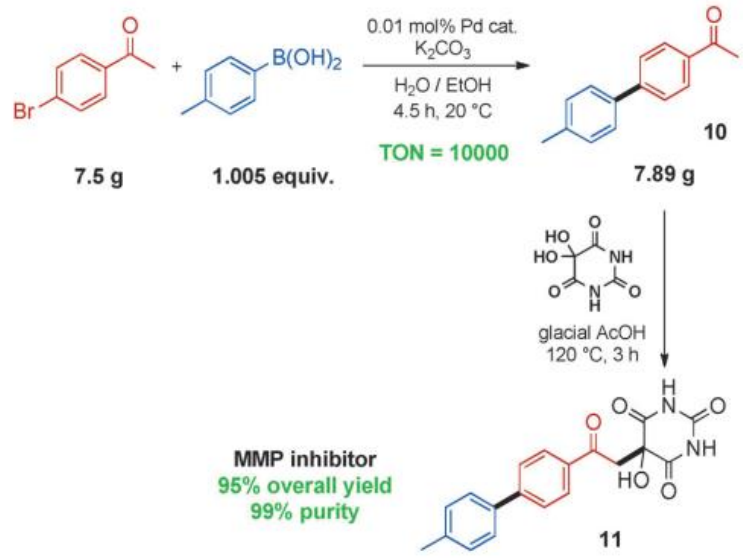

Scheme 10. Synthesis of MMP inhibitor. Adapted from ref.[97]

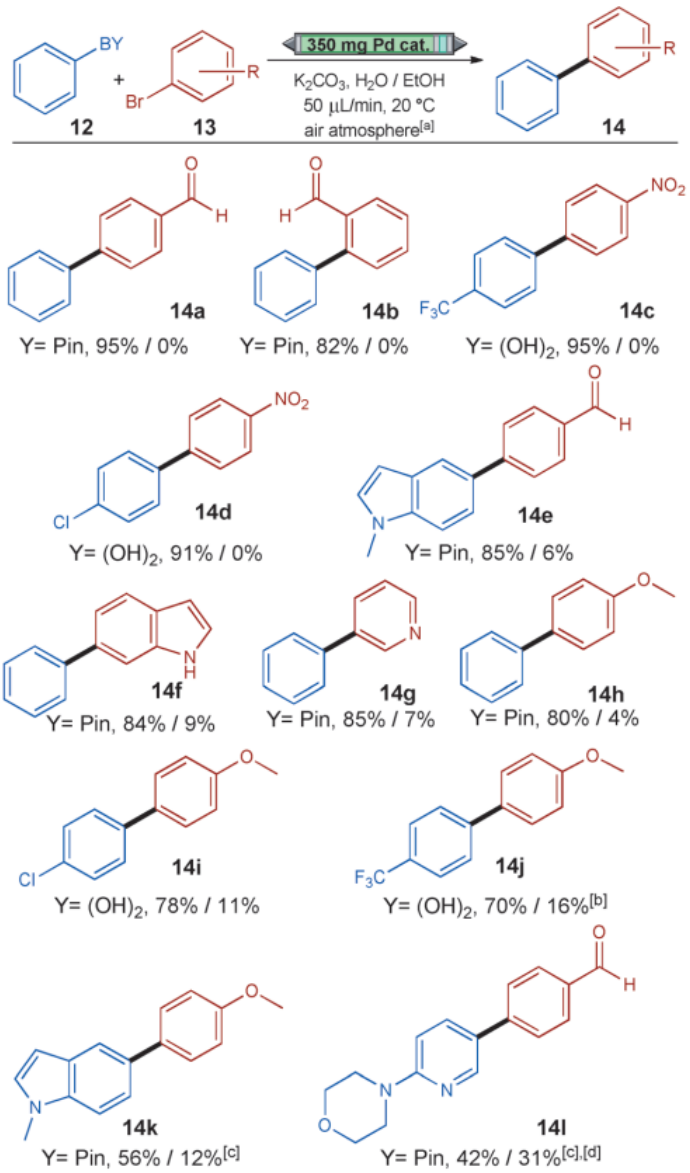

Scheme 9. Synthesis of a mini-library of coupling products in one continuous flow experiment. [a] Products listed in the order they were synthesized. Left: Isolated yields reported. Right: by-products determined by 1H NMR spectroscopy from crude reaction mixtures. [b] Outflowing solution slightly yellow. [c] Outflowing solution strongly yellow. [d] Product not isolated. Pin: pinacolate. Reproduced with permission of ref.[97] Copyright 2015 Wiley.

Very recently, a promising approach was designed for the preparation of core shell NH_2-MIL-101(Fe)@Pd@COFs catalyst by encapsulating MOFs in COFs with different pore sizes (Figure 18).[99] Among NH_2-MIL-101(Fe)@Pd@COFs(3+2) and NH_2-MIL-101(Fe)@Pd@COFs (3 + 3) catalysts, the later solid exhibits high stability, nice morphology, Fe-based electron transfer synergy and highly dispersed Pd NPs. However, the size of the Pd NPs was similar in these two catalysts as shown by TEM. The activity of NH_2-MIL-101(Fe)@Pd@COFs(3 + 3) and NH_2-MIL-101(Fe)@Pd@COFs(3 + 2) solids was tested in the Suzuki-Miyaura coupling reaction between iodobenzene and phenylboronic acid using TEA as a base in water at 50 °C in 5 h. The biphenyl yield was 99 and 75% with NH_2-MIL-101(Fe)@Pd@COFs(3 + 3) and NH_2-MIL-101(Fe)@Pd@COFs(3 + 2) solids, respectively

under these conditions. The catalyst was recycled five times with a slight reduction in the catalytic activity. This decreased activity was believed due to the oxidation of Pd NPs.

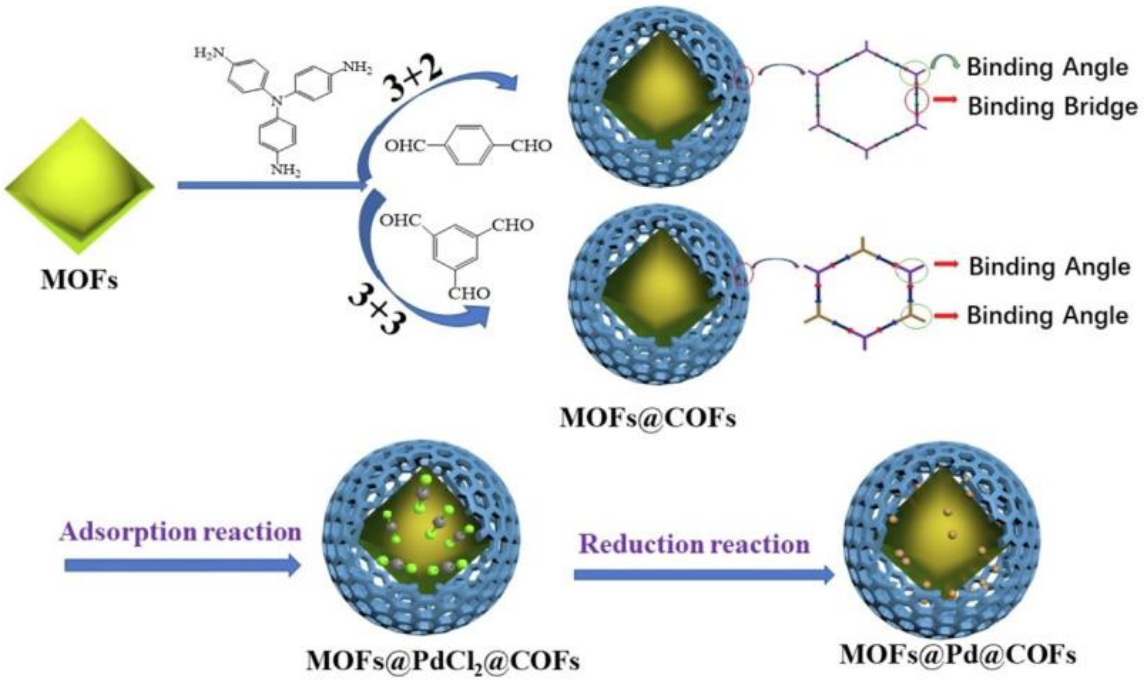

Figure 18. Synthetic schematic for the fabrication of MOFs@Pd@COFs. Reproduced with permission of ref.[99] Copyright 2022 Elsevier.

A mixed linker two-dimensional desolvated MOF, $\{[Cu(1,2,3\text{-btc})(bpe)(H_2O)]\cdot H_2O\}_n$ (Cu-MOF) (btc: 1,2,3-benzenetricarboxylate; bpe: 1,2-bis(4-ypridyl) ethane) was employed as a support for the stabilization of Pd NPs (2-3 nm) through the non-coordinated carboxylate groups available within the pore surface (Figure 19).[100] The catalytic performance of Pd@Cu-MOF was tested in the Suzuki-Miyaura coupling reaction between phenylboronic acid and iodobenzene using Cs_2CO_3 in THF at 60 ^oC in 24 h showing 99% yield of biphenyl. Further, Pd@Cu-MOF solid was active in promoting Suzuki-Miyaura coupling with different aryl halides in high yields. Also, the activity of Pd@Cu-MOF was identical with no decrease in the yield of biphenyl up to four cycles. TEM images revealed no considerable agglomeration of Pd NPs while powder XRD suggested similar diffraction peaks after four cycles, however, slight broadening of the peaks was also observed.

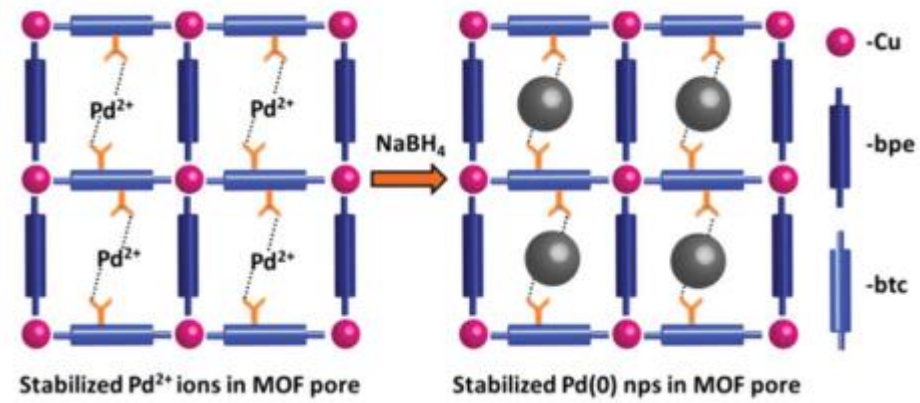

Figure 19. Schematic diagram showing the interaction of the pendent 'COOH' groups with the Pd NPs in the MOF pore and the stabilization. Reproduced with permission of ref.[100] Copyright 2019 Royal Society of Chemistry.

Pd NPs (1.8 nm) were immobilized over HKUST-1 to obtain Pd@HKUST-1 and its catalytic activity was tested in the Suzuki-Miyaura coupling reaction through one-pot tandem procedure.[101] Initially, phenylboronic acid was reacted with iodine to give the corresponding iodoarene which were later reacted with phenylboronic acid to provide the expected biphenyl product. Under the optimized reaction conditions, the reaction of phenylboronic acid with iodine in the presence of Pd@HKUST-1 using K_2CO_3 as a base in ethanol at 70 ^oC under N_2 atmosphere in 7 h showed 81% yield of biphenyl. A series of biphenyl derivatives was prepared by adopting this procedure with moderate to high yields under these conditions. The stability of Pd@HKUST-1 was checked with 3-chlorophenylboronic acid and the yields were maintained even after 5 cycles of reuse. Also, powder XRD patterns of the reused solid showed no changes in the crystallinity compared to the fresh solid.

Pd NPs were deposited over MOF-199 to obtain Pd@MOF-199 and the activity of the later solid was examined in the Suzuki-Miyaura coupling reaction between bromobenzene and phenylboronic acid in the presence of Pd@MOF-199 using K_2CO_3 as a base in H_2O/EtOH (1:2) mixture at 60 ^oC after 5 h.[102] Among the various conditions optimized, the yield of biphenyl was 92% under the above conditions. Further, a series of biphenyl derivatives were also synthesised using Pd@MOF-199 as a heterogeneous catalyst under the optimized conditions. The solid was used for five cycles with a slight decrease in the yield, while, no significant leaching of Pd was observed.

Recently, an elegant approach was designed to inhibit the shrinkage of mesopores in MOFs and to increase the internal surface area by introducing small quantities of polymer. In this way, the accessible surface areas in the modified MOFs are enhanced significantly from 5 to 50 times since the incorporated polymer effectively pins the MOFs open.[103] In this connection, an isostructural MOFs, M_2(NDISA) (where M = Ni^{2+}, Co^{2+}, Mg^{2+}, or Zn^{2+}) (NDISA: naphthalene-1,4,5,8-tetracarboxylic dianhydride) were selected as suitable hosts to introduce polydopamine (PDA) to prepare series of MOF−polymer composites [M_2(NDISA)-PDA]. Thus, Pd NPs (2 nm) were immobilized within the pores of these composites to afford M_2(NDISA)-PDA-Pd (Figure 20). The activity of the later solid was tested in the Suzuki-Miyaura coupling reaction between aryl halide, phenylboronic acid using K_2CO_3 as a base in DMF-H_2O (1:1) at 50 ^oC. The Suzuki-Miyaura coupling between 4-iodotoluene and phenylboronic acid in the presence of Ni_2(NDISA)-PDA-Pd provided 48% yield in 5 min with a TOF value of 5760 h^{-1}. This activity is superior than the state-of-the-art homogeneous $Pd(PPh_3)_2Cl_2$ catalyst.[104] Under identical conditions, Ni_2(NDISA) showed no activity for this reaction and PDA-Pd gave only 3% yield after 3 h and this poor activity is due to the low surface area (7 m_2/g). Interestingly, the activity of Ni_2(NDISA)-Pd (without PDA) was 83% after 3 h while Ni_2(NDISA)-PDA-Pd required only 1 h to afford 83% yield. The superior performance of Ni_2(NDISA)-PDA-Pd catalyst compared to other solids was ascribed due to (1) The higher pore volume and surface area provided by Ni_2(NDISA)-PDA-Pd composite favours mass transfer inside the MOF channels; (2) the high density of coordinating functional groups on the PDA backbone facilitates the deposition of ultrasmall Pd NPs with high dispersion thus providing high density of active sites and (3) PDA in the composite can also behave as a reducing agent to endows the Pd clusters with very clean surfaces for a catalytic reaction. However, reusability data to ascertain catalyst stability were not reported.

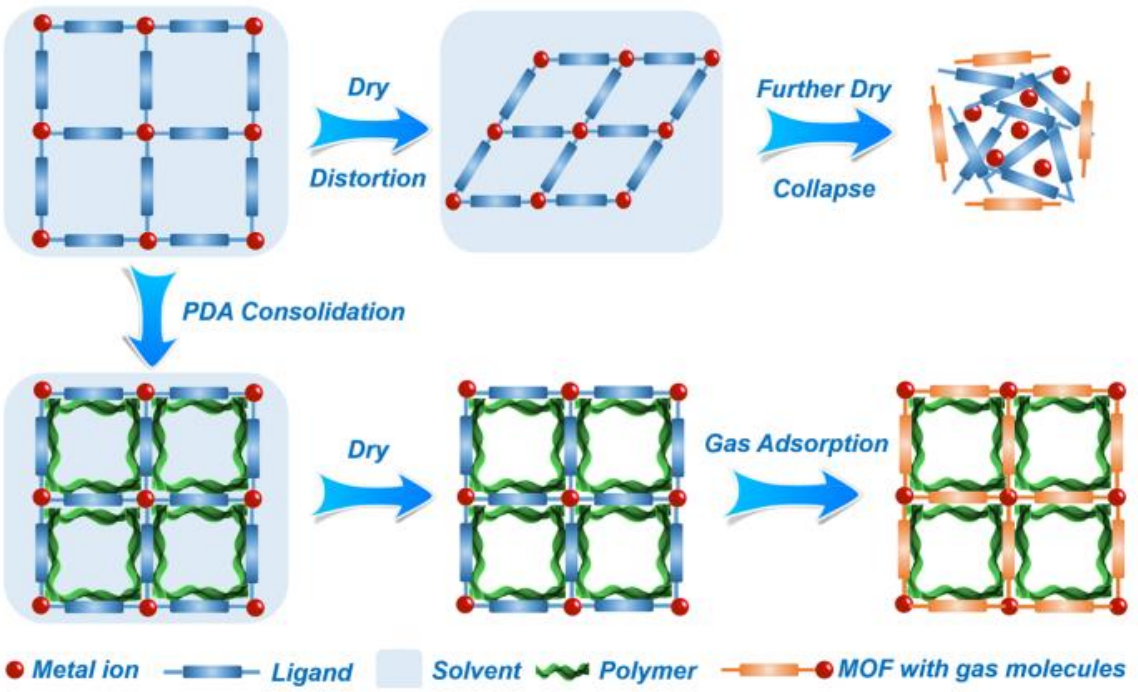

Figure 20. Polymer introduced into the pore channel supports the porous structure and prevents the mesopores from collapsing, leaving the pores accessible to gas molecules. Reproduced with permission of ref.[103] Copyright 2019 American Chemical Society.

Ultrasmall thiolated Pd nanoclusters (Pd_n(l-Cys)$_m$) were immobilized inside the cavities of Ce-MOF-808, CeUiO-66 and Ce-BTC and the resulting Pd_n@Ce-MOF-808, Pd_n@CeUiO-66 and Pd_n@Ce-BTC solids activity was tested in the Suzuki-Miyaura coupling between phenylboronic acid and bromobenzene in EtOH:H_2O (1:1) using K_2CO_3 as a base with microwave irradiation for 5 min at 80 ^oC.[105] Pd_n@Ce-MOF-808 exhibited the highest TOF value of (132530 h^{-1}) for the above reaction under these conditions while Pd_n@Ce-UiO-66 and Pd_n@Ce-BTC resulted in TOF values of 123924 and 110155 h^{-1}, respectively under the above conditions. The high remarkable catalytic activity of Pd_n@Ce-MOF-808 was due to the unique atomic packing structure and electronic properties of the Pd nanoclusters and the high porosity/surface area of this MOF structure. Furthermore, Pd_n@Ce-MOF-808 was recycled in at least five times without significant loss of activity. HRTEM images revealed that the Pd nanoclusters size remained unaltered during reusability.

We have compared the activity and stability of the Pd sites using different chelating groups in the different MOFs reviewed here (see Table 1), taking the Suzuki-Miyaura coupling as a test reaction.

Table 1. Catalytic performance of different Pd-based MOFs for the Suzuki-Miyaura cross coupling reaction.

MOF	Pd source	Location	TON/ TOF (h^{-1})	Nº reuses/Pd leached	Ref.
Molecular Pd					
MIL-101	$Na_2(PdCl_4)$	Pores	1620/1820	6/ 2%	[53]
$[Pd(2\text{-pymo})_2]_n$	$K_2(PdCl_4)$	Nodes	34/1230	1/-	[58]

UiO-67-bipy	$PdCl_2(CH_3CN)_2$	Linker	9040/1970	10/5%	[67]
IRMOF-3-SA[a]	$Pd(OAc)_2$	Linker	846/170	5/<0.5%	[78]
MIL-101-NHC	$Pd(OAc)_2$	Linker	108/-	5/<4%	[81]
Pd NPs					
Au/Pd@UiO-66-NH_2 (6.45 nm)	$HAuCl_4$, Na_2PdCl_4	MOF surface	-/426	3/-	[87]
UiO-66-NH_2-Gl@Pd (10 nm)	$PdCl_2$	MOF surface	1900/3800	4/-	[89]
Pd_1/Ni_4-MOF@PAN(C)	$Ni(NO_3)_2{\cdot}6H_2O$, $Pd(NO_3)_2{\cdot}2H_2O$	MOF surface	-/717	6/-	[92]
Pd@MIL-101(Cr)-NH_2 (2.6 nm)	$PdCl_2(MeCN)_2$	MOF surface	-/-	10/-	[95]
Pd_n@Ce-MOF-808	K_2PdCl_4	MOF surface	-/132530	5/-	[105]

[a]salicylaldehyde

5. Conclusions

The use of MOFs as support of Pd active sites is a feasible strategy that results in the multiplication of turnovers with respect to the homogeneous counterparts, allowing the simple recovery and recycle with minimum leaching of Pd. This has been proven in proof-of-concept Suzuki-Miyaura and Heck type C-C couplings of different substrates under different conditions, indicating the robustness of those systems. Among them, the isolation of Pd(II) sites at the organic linkers represents the bridging between homogeneous organometallic Pd complexes and supported Pd catalysts. Indeed, Pd (II) catalysts are readily available for the cleavage of C-H and C-X (X = Cl, Br, I, $B(OH)_2$) bonds and formation of key aryl/alkyl-Pd(II) intermediates that leads to the formation of the C-C bond.

In the case of the immobilization of molecular Pd complexes, the activity of linker/node/pore functionalized MOFs has been proved to be higher than that of the homogeneous Pd salt employed as precursor, especially when accounting the large number of recycles (up to 10), which multiplied the TON values. The amount of Pd leached is also significantly reduced (<10% of the total Pd), with respect to the 100% Pd leached in the case of the homogeneous catalyst. Remarkable performance in terms of activity increase and reusability have been achieved when using electro-donating N/O-containing groups at the MOF linker, such as bipyridine or Schiff base, in contrast to more labile Pd inclusion into the pore or by interaction/exchange with the inorganic nodes. However, in this later case the electrophilicity of Pd is maintained to a higher extent, thus increasing its reactivity at expense

of its stability. One of the major routes of Pd(II) deactivation is its redaction to Pd(0) aggregates during the catalytic cycle, which highlights the importance of chelating, immobilize and isolate those electrophilic Pd sites, as well as the use of oxidants to reverse the reduction process of the active sites. This have been already demonstrated in oxidative Heck type C-C coupling starting from non-functionalized C-H bonds, giving a simple and less expensive methodology than the use of boronic acids or aryl halide precursors.

On the other hand, Pd nanoparticles have been a widely used catalytic system for C-C couplings during the last decades due to their large surface areas and ratio of atoms remaining in the surface of the nanoparticle. Pd NPs have been deposited in wide range of MOFs and their activity data are highly promising compared to homogeneous catalysts. One of the crucial issues in this case is to control the particle size and to encapsulate within the pores of MOFs. If the Pd particle size is larger than the pores of MOFs, then, these NPs exist mostly on the outer surface of the MOF solid, showing high activity in few cycles. Later, the activity of this solid is decreased due to the leaching and agglomeration of Pd NPs (lack of confinement). As discussed earlier, the selection of a base is highly important for these C-C coupling reactions, but sufficient care should also be given to maintain MOF stability. After demonstrating the unique features and merits of Pd NPs encapsulated over MOFs, the next target in this field is to use them as solid heterogeneous catalyst for the preparation of natural products employing these C-C coupling reactions. Furthermore, the activity of Pd NPs deposited over two-dimensional MOFs is also not explored. These solids would be ideal candidates to stabilize Pd NPs as well as to enhance the diffusion of bulkier organic molecules due to the two-dimensional nature of MOFs. Thus, it is strongly believed that this filed will be expanding in new dimensions in the near future with the development of new MOF-based Pd catalysts for challenging natural product synthesis.

As we have commented, both molecular Pd complexes and nanoparticles have their own advantages and disadvantages. In theory, the Pd(II) molecular catalysts have a higher reactivity with unprecedented TON/TOF values due to their discrete and isolated nature (as well as the low metal loading). In contrast, larger amount of metal is often present in the Pd nanoparticles and only the atoms on the surface participate in the catalytic cycle. However, the synthesis of metal nanoparticles is often simple, ligandless and inexpensive, while the grafting strategy of molecular Pd species to the MOF is often costly, challenging and leaching or Pd aggregation/sintering into large particles may occur when the bonding to the MOF is not sufficiently strong. Moreover, too strong Pd-MOF bonding may lead to inactivation of the active sites, blocking the formation of key Pd-substrate reaction intermediates. In contrast, the nanoparticle size can be controlled by the use of ordered porous systems that blocks the Pd nanoparticle growing to an optimal size for enhancing its activity while minimizing the leaching of soluble Pd(II) species. Regarding selectivity, the linker employed for the coordination of Pd can be used to control the activation of the substrate towards the desired product, resulting in shape-selectivity. In this sense, the incorporation of Pd nanoparticles in the MOF pores may plug them and decrease the available surface area of the supported catalyst, in contrast to the small size of discrete molecular Pd complexes, which maintain the available microporous space in the MOF in order to favour the diffusion of reagents and products.

In this context, the new directions in the field of Pd-grafted on MOF (either in the form of molecular species or nanoparticles) to overcome such challenges are to develop:

- High surface MOF supports with tuneable polarity and metal-support interactions to increase the dispersion and isolation of the grafted Pd catalyst, which allow to decrease the loading and thus the cost of the precious metal catalyst.
- Functional groups for the strong bonding of Pd sites, either at the linker or nodes of the MOF, to increase the stability during the Pd(0/II) catalytic cycle, avoid leaching of active sites and improve the recycling of the grafted catalyst.
- Redox-active MOFs for the re-oxidation of Pd(0) to Pd(II) and improve the number of turnovers and catalyst life time in the presence of benign oxidants (e.g. oxygen) under mild conditions.
- New Pd-MOF catalyzed C-H activation strategies for C-C bond formations from non-functionalized substrates, which provides step and atom-economy, cleaner synthesis and avoids the use of stoichiometric base and formation of byproducts.
- Finely tuned MOF cavities and pores for shape-selective-catalysis to increase the regio-selectivity when different C-C bond formations may occur, by using different synthetic approach (new linkers, metals and MOF crystalization conditions).
- Multi-metal and mix-linker MOFs will result in multifunctional MOF crystals with synergic and unprecedented selectivities, modulating the electronic and steric environment of the Pd sites for improved activity and stability.

Acknowledgements

AD thanks the University Grants Commission, New Delhi, for the award of an Assistant Professorship under its Faculty Recharge Programme. ASL and BS thank DST-PURSE for providing financial support for the purchase of work station. The project that gave rise to these results received the support of a fellowship from ”la Caixa” Foundation (ID 100010434). The fellowship code is LCF/BQ/PI19/11690011”. F. G: Cirujano also acknowledges the “Ramon y Cajal” contract with code RYC2020-028681-I. N. Martín acknowledges the “Juan de la Cierva formación” fellowship with code FJC2018-035455-I.

References

[1] A. Suzuki, *J. Organomet. Chem.* **1999**, *576*, 147.
[2] R. Martin, S. L. Buchwald, *Acc. Chem. Res.* **2008**, *41*, 1461.
[3] C. C. C. Johansson Seechurn, M. O. Kitching, T. J. Colacot, V. Snieckus, *Angew. Chem. Int. Ed.* **2012**, *51*, 5062.
[4] S. Kotha, K. Lahiri, D. Kashinath, *Tetrahedron* **2002**, *58*, 9633.
[5] A. F. Littke, C. Dai, G. C. Fu, *J. Am. Chem. Soc.* **2000**, *122*, 4020.
[6] A. Suzuki, *Angew. Chem. Int. Ed.* **2011**, *50*, 6722.
[7] C. Torborg, M. Beller, *Adv. Synth. Catal.* **2009**, *351*, 3027.
[8] S. R. Chemler, D. Trauner, S. J. Danishefsky, *Angew. Chem. Int. Ed.* **2001**, *40*, 4544.
[9] A. Biffis, P. Centomo, A. D. Zotto, M. Zecca, *Chem. Rev.* **2018**, *118*, 2249.
[10] N. Miyaura, A. Suzuki, *Chem. Rev.* **1995**, *95*, 2457.
[11] F.-S. Han, *Chem. Soc. Rev.* **2013**, *42*, 5270.
[12] E.-I. Negishi, *Angew. Chem. Int. Ed.* **2011**, *50*, 6738.
[13] S. R. Dubbaka, P. Vogel, *Angew. Chem. Int. Ed.* **2005**, *44*, 7674.
[14] H. Li, C. C. C. Johansson Seechurn, T. J. Colacot, *ACS Catal.* **2012**, *2*, 1147.
[15] M.-J. Jin, D.-H. Lee, *Angew. Chem. Int. Ed.* **2010**, *49*, 1119.

[16] O. Navarro, N. Marion, J. Mei, S. P. Nolan, *Chem. Eur. J.* **2006**, *12*, 5142.
[17] J. Zhou, G. C. Fu, *J. Am. Chem. Soc.* **2004**, *126*, 1340.
[18] C. M. Crudden, M. Sateesh, R. Lewis, *J. Am. Chem. Soc.* **2005**, *127*, 10045.
[19] V. Polshettiwar, C. Len, A. Fihri, *Coord. Chem. Rev.* **2009**, *253*, 2599.
[20] A. R. Siamaki, A. E. R. S. Khder, V. Abdelsayed, M. S. El-Shall, B. F. Gupton, *J. Catal.* **2011**, *279*, 1.
[21] J.-H. Kim, J.-W. Kim, M. Shokouhimehr, Y.-S. Lee, *J. Org. Chem.* **2005**, *70*, 6714.
[22] S. Ogasawara, S. Kato, *J. Am. Chem. Soc.* **2010**, *132*, 4608.
[23] Y. Monguchi, T. Ichikawa, T. Yamada, Y. Sawama, H. Sajiki, *Chem. Rec.* **2019**, *19*, 3.
[24] N. T. S. Phan, M. V. Der Sluys, C. W. Jones, *Adv. Synth. Catal* **2006**, *348*, 609.
[25] M. Pagliaro, V. Pandarus, R. Ciriminna, F. Béland, P. D. Carà, *ChemCatChem* **2012**, *4*, 432.
[26] H. Furukawa, K. E. Cordova, M. O'Keeffe, O. M. Yaghi, *Science* **2013**, *341*, 1230444.
[27] M. Li, D. Li, M. O'Keeffe, O. M. Yaghi, *Chem. Rev.* **2014**, *114*, 1343.
[28] H. Li, M. Eddaoudi, M. O'Keeffe, O. M. Yaghi, *Nature* **1999**, *402*, 276.
[29] H. K. Chae, D. Y. Siberio-Pérez, J. Kim, Y. B. Go, M. Eddaoudi, A. J. Matzger, M. O'Keeffe, O. M. Yaghi, *Nature* **2004**, *427*, 523.
[30] S. Kitagawa, R. Kitaura, S.-I. Noro, *Angew. Chem. Int. Ed.* **2004**, *43*, 2334.
[31] A. Corma, H. García, F. X. Llabrés I Xamena, *Chem. Rev.* **2010**, *110*, 4606.
[32] S. Horike, M. Dincă, K. Tamaki, J. R. Long, *J. Am. Chem. Soc.* **2008**, *130*, 5854.
[33] F. G. Cirujano, F. X. Llabrés I Xamena, *J. Phys. Chem. Lett.* **2020**, *11*, 4879.
[34] S. Oudi, A. R. Oveisi, S. Daliran, M. Khajeh, E. Teymoori, *J. Colloid Interf. Sci.* **2020**, *561*, 782.
[35] L. Zhu, X.-Q. Liu, H.-L. Jiang, L.-B. Sun, *Chem. Rev.* **2017**, *117*, 8129.
[36] A. Dhakshinamoorthy, N. Heidenreich, D. Lenzen, N. Stock, *CrystEngComm* **2017**, *19*, 4187.
[37] S. T. Meek, J. A. Greathouse, M. D. Allendorf, *Adv. Mater.* **2011**, *23*, 249.
[38] A. Dhakshinamoorthy, H. Garcia, *Chem. Soc. Rev.* **2012**, *41*, 5262.
[39] H.-L. Jiang, Q. Xu, *Chem. Commun.* **2011**, *47*, 3351.
[40] Q.-L. Zhu, J. Li, Q. Xu, *J. Am. Chem. Soc.* **2013**, *135*, 10210.
[41] C. Wu, F. Irshad, M. Luo, Y. Zhao, X. Ma, S. Wang, *ChemCatChem* **2019**, *11*, 1256.
[42] M. Kaur, S. Kumar, S. A. Younis, M. Yusuf, J. Lee, S. Weon, K.-H. Kim, A. K. Malik, *Chem. Eng. J.* **2021**, *423*, 130230.
[43] A. Dhakshinamoorthy, A. M. Asiri, H. García, *Trends Chem.* **2020**, *2*, 454.
[44] S. M. Cohen, *Chem. Rev.* **2012**, *112*, 970.
[45] Z. Yin, S. Wan, J. Yang, M. Kurmoo, M.-H. Zeng, *Coord. Chem. Rev.* **2019**, *378*, 500.
[46] D. Jiang, L. L. Keenan, A. D. Burrows, K. J. Edler, *Chem. Commun.* **2012**, *48*, 12053.
[47] T. Drake, P. Ji, W. Lin, *Acc. Chem. Res.* **2018**, *51*, 2129.
[48] S. Rostamnia, H. Alamgholiloo, X. Liu, *J. Colloid Interf. Sci.* **2016**, *469*, 310.
[49] S.-N. Kim, S.-T. Yang, J. Kim, J.-E. Park, W.-S. Ahn, *CrystEngComm* **2012**, *14*, 4142.
[50] N. Martín, F. G. Cirujano, *Org. Biomol. Chem.*, *18* 8058.
[51] A. Dhakshinamoorthy, A. M. Asiri, H. Garcia, *Chem. Soc. Rev.* **2015**, *44*, 1922.
[52] T.-H. Park, A. J. Hickman, K. Koh, S. Martin, A. G. Wong-Foy, M. S. Sanford, A. J. Matzger, *J. Am. Chem. Soc.* **2011**, *133*, 20138.
[53] S. Rezaei, A. Landarani-Isfahani, M. Moghadam, S. Tangestaninejad, V. Mirkhani, I. Mohammadpoor-Baltork, *RSC Adv.* **2016**, *6*, 92463.
[54] S. Tarnowicz-Ligus, A. Augustyniak, A. M. Trzeciak, *Eur. J. Inorg. Chem.* **2019**, 4282.
[55] I. Ioannis Anastasiou, N. V. Niels Van Velthoven, E. Elena Tomarelli, A. Aurora Lombi, D. Daniela Lanari, P. Pei Liu, S. Sara Bals, D. E. Dirk E. De Vos, L. Luigi Vaccaro, *ChemSusChem* **2020**, *13*, 2786
[56] F. G. Cirujano, P. Leo, J. Vercammen, S. Smolders, G. Orcajo, D. E. De Vos, *Adv. Synth. Catal.* **2018** *360*, 3872.
[57] A. Valiente, S. Carrasco, A. Sanz-Marco, C.-W. Tai, A. B. Bermejo Gómez, B. Martín-Matute, *ChemCatChem* **2019**, *11*, 3933.

[58] F. X. Llabrés i Xamena, A. Abad, A. Corma, H. Garcia, *J. Catal.* **2007**, *250* 294.
[59] J. A. R. Navarro, E. Barea, J. M. Salas, N. Masciocchi, S. Galli, A. Sironi, C. O. Ania, J. B. Parra, *Inorg. Chem.* **2006**, *45*, 2397.
[60] Y. Liu, J. Wang, T. Li, Z. Zhao, W. Pang, *Tetrahedron* **2019**, *75* 130540.
[61] L.-X. You, L.-X. Cui, B.-B. Zhao, G. Xiong, F. Ding, B.-Y. Ren, Z.-L. Shi, I. Dragutan, V. Dragutan, Y.-G. Sun, *Dalton Trans.* **2018**, *47*, 8755.
[62] N. V. Velthoven, S. Waitschat, S. M. Chavan, P. Liu, S. Smolders, J. Vercammen, B. Bueken, S. Bals, K. P. Lillerud, N. Stock, D. E. De Vos, *Chem. Sci.* **2019**, *10*, 3616.
[63] K.-I. Otake, J. Ye, M. Mandal, T. Islamoglu, C. T. Buru, J. T. Hupp, M. Delferro, D. G. Truhlar, C. J. Cramer, O. K. Farha, *ACS Catal.* **2019**, *9*, 5383−5390.
[64] J. Huang, W. Wang, H. Li, *ACS Catal.* **2013**, *3*, 1526−1536.
[65] N.-X. Zhu, Z.-W. Wei, C.-X. Chen, D. Wang, C.-C. Cao, Q.-F. Qiu, J.-J. Jiang, H.-P. Wang, C.-Y. Su, *Angew. Chem. Int. Ed.* **2019**, *58*, 17033.
[66] C. Bai, S. Jian, X. Yao, Y. Li, *Catal. Sci. Technol.* **2014**, *4*, 3261.
[67] S. Kim, S. Jee, K. M. Choi, D.-S. Shin, *Nano Res.* **2021**, *14*, 486.
[68] X.-F. Gong, L.-Y. Zhang, H.-X. Zhang, Y.-M. Cui, F.-C. Jin, Y. Liu, Y.-F. Zhai, J.-H. Li, G.-Y. Liu, Y.-F. Zeng, *Anorg. Allg. Chem.* , **2020**, 1336.
[69] L. Chen, S. Rangan, J. Li, H. Jiang, Y. Li, *Green Chem.* **2014**, *16*, 3978.
[70] R. V. Zeeland, X. Li, W. Huang, L. M. Stanley, *RSC Adv.* **2016**, *6*, 56330.
[71] S. Jia, X. Xiao, Q. Li, Y. Li, Z. Duan, Y. Li, X. Li, Z. Lin, Y. Zhao, W. Huang, *Inorg. Chem.* **2019**, *58*, 12748−12755.
[72] W. Chen, P. Cai, P. Elumalai, P. Zhang, L. Feng, M. Al-Rawashdeh, S. T. Madrahimov, H.-C. Zhou, *ACS Appl. Mater. Interfaces* **2021**, *13*, 51849−51854.
[73] D. Dong, Z. Li, D. Liu, N. Yu, H. Zhao, H. Chen, J. Liu, D. Liu, *New J. Chem.* **2018**, *42*, 9317.
[74] H. Veisi, M. Abrifam, S. A. Kamangar, M. Pirhayati, S. G. Saremi, M. Noroozi, T. Tamoradi, B. Karmakar, *Sci.Rep* **2021**, *11*, 21883.
[75] G. Xiong, X.-L. Chen, L.-X. You, B.-Y. Ren, F. Ding, I. Dragutan, V. Dragutan, Y.-G. Sun, *Journal of Catalysis 361 (2018) 116-125*.
[76] S. Rostamnia, H. Alamgholiloo, X. Liu, *J. Colloid Interf. Sci.* **2016**, *469* 310.
[77] B. Salahshournia, H. Hamadi, V. Nobakht, *Polyhedron* **2020**, *189* 114749.
[78] F. Nouri, S. Rostamizadeh, M. Azad, *Mol. Catal.* **2017**, *443* 286.
[79] J. Lim, S. Lee, H. Ha, J. Seong, S. Jeong, M. Kim, S. B. Baek, M. S. Lah, *Angew. Chem. Int. Ed.* **2021**, *60*, 9296.
[80] R. Sen, D. Saha, S. Koner, P. Brando, Z. Lin, *Chem. Eur. J.* **2015**, *21*, 5962.
[81] E. Niknam, F. Panahi, A. Khalafi-Nezhad, *J. Organomet. Chem.* **2021**, *935* 121676.
[82] M. Bahadori, S. Tangestaninejad, M. Moghadam, V. Mirkhani, A. Mechler, I. Mohammadpoor-Baltork, F. Zadehahmadi, *Micropor. Mesopor. Mater.* **2017**, *253* 102.
[83] Y.-L. Wei, Y. Li, Y.-Q. Chen, Y. Dong, J.-J. Yao, X.-Y. Han, Y.-B. Dong, *Inorg. Chem.* **2018**, *57*, 4379−4386.
[84] C. I. Ezugwu, B. Mousavi, M. A. Asraf, Z. Luo, F. Verpoort, *J. Catal.* **2016**, *344* 445.
[85] M. Zhang, J. Guan, B. Zhang, D. Su, C. T. Williams, C. Liang, *Catal. Lett.* **2012**, *142*, 313.
[86] S. Gao, N. Zhao, M. Shu, S. Che, *Appl. Catal. A: Gen.* **2010**, *388* 196.
[87] S. Subudhi, S. Mansingh, S. P. Tripathy, A. Mohanty, P. Mohapatra, D. Rath, K. Parida, *Catal. Sci. Technol.* **2019**, *9*, 6585.
[88] L. Cheng, K. Zhao, Q. Zhang, Y. Li, Q. Zhai, J. Chen, Y. Lou, *Inorg. Chem.* **2020**, *59*, 7991−8001.
[89] H. Alinezhad, M. Cheraghian, S. Ghasemi, *J. Organomet. Chem.* **2020**, *907* 121069.
[90] X. Li, B. Zhang, R. V. Zeeland, L. Tang, Y. Pei, Z. Qi, T. W. Goh, L. M. Stanley, W. Huang, *Catal. Lett.* **2018**, *148*, 940.
[91] Y. Huang, S. Gao, T. Liu, J. Lu, X. Lin, H. Li, R. Cao, *ChemPlusChem* **2012**, *77*, 106.
[92] Y. Su, Y. Zhang, C. Li, G. Xu, J. Bai, *Catal. Lett.* **2020**, *150*, 3196.

[93] A. W. Augustyniak, W. Zawartka, J. A. R. Navarro, A. M. Trzeciak, *Dalton Trans.* **2016**, *45*, 13525.
[94] J. Wang, T. Li, Z. Zhao, X. Zhang, W. Pang, *Catal Lett* **2021**, 10.1007/s10562.
[95] V. Pascanu, Q. Yao, A. B. Gmez, M. Gustafsson, Y. Yun, W. Wan, L. Samain, X. Zou, B. Martin-Matute, *Chem. Eur. J.* **2013**, *19*, 17483.
[96] F. Carson, V. Pascanu, A. B. Gûmez, Y. Zhang, A. E. Platero-Prats, X. Zou, B. Martin-Matute, *Chem. Eur. J.* **2015**, *21*, 10896.
[97] V. Pascanu, P. R. Hansen, A. B. Gmez, C. Ayats, A. E. PlateroPrats, M. J. Johansson, M. A. Pericas, B. Martin-Matute, *ChemSusChem* **2015**, *8*, 123.
[98] O. Nicolotti, M. Catto, I. Giangreco, M. Barletta, F. Leonetti, A. Stefanachi, L. Pisani, S. Cellamare, P. Tortorella, F. Loiodice, A. Carotti, *Eur. J. Med. Chem.* **2012**, *58*, 368.
[99] C. Mao, K. Yin, C. Yang, G. Dong, G. Tian, Y. Zhang, Y. Zhou, *J. Colloid Interf. Sci.* **2022**, *608*, 809.
[100] S. A. Adalikwu, V. S. Mothika, A. Hazra, T. K. Maji, *Dalton Trans.* **2019**, *48*, 7117.
[101] H. Tang, M. Yang, X. Li, M.-L. Zhou, Y.-S. Bao, X.-Y. Cui, K. Zhao, Y.-Y. Zhang, Z.-B. Han, *Inorg. Chem. Commun.* **2021**, *123* 108368.
[102] M. Sanaei, R. Fazaeli, H. Aliyan, *J. Chin. Chem. Soc.* **2019**, *66*, 1290.
[103] L. Peng, S. Yang, S. Jawahery, S. M. Moosavi, A. J. Huckaba, M. Asgari, E. Oveisi, M. K. Nazeeruddin, B. Smit, W. L. Queen, *J. Am. Chem. Soc.* **2019**, *141*, 12397.
[104] S. Lu, Y. Hu, S. Wan, R. McCaffrey, Y. Jin, H. Gu, W. Zhang, *J. Am. Chem. Soc.* **2017**, *139*, 17082−17088.
[105] M. Farrag, *Micropor. Mesopor. Mater.* **2021**, *312* 110783.